A MODEL FOR PALLADIUM CATALYZED DESTRUCTION OF CHLORINATED ETHENE CONTAMINATED GROUNDWATER

Chris M. Stoppel, Captain, USAF

AFIT/GEE/ENV/01M-21

DEPARTMENT OF THE AIR FORCE
AIR UNIVERSITY
AIR FORCE INSTITUTE OF TECHNOLOGY

Wright-Patterson Air Force Base, Ohio

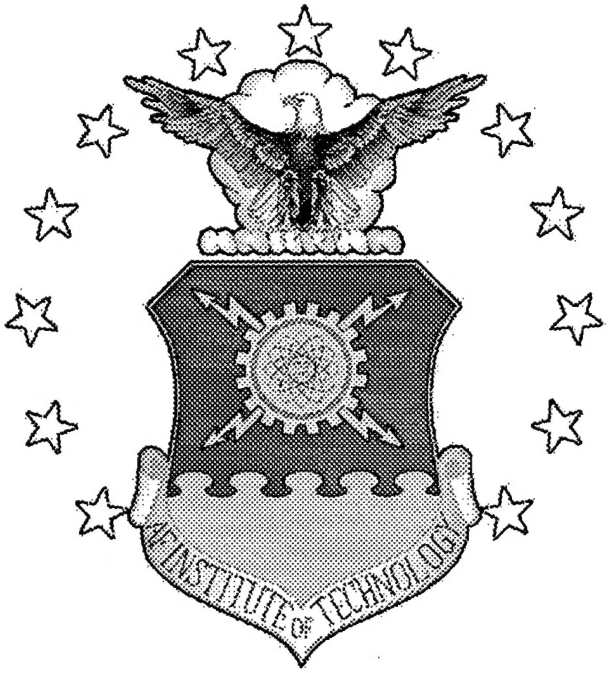

A MODEL FOR PALLADIUM CATALYZED DESTRUCTION OF CHLORINATED ETHENE CONTAMINATED GROUNDWATER

Chris M. Stoppel, Captain, USAF

AFIT/GEE/ENV/01M-21

DEPARTMENT OF THE AIR FORCE
AIR UNIVERSITY
AIR FORCE INSTITUTE OF TECHNOLOGY

Wright-Patterson Air Force Base, Ohio

The views expressed in this thesis are those of the author and do not reflect the official policy or position of the United States Air Force, Department of Defense, or the U. S. Government.

AFIT/GEE/ENV/01M-21

A MODEL FOR PALLADIUM CATALYZED DESTRUCTION OF CHLORINATED ETHENE CONTAMINATED GROUNDWATER

THESIS

Presented to the Faculty

Department of Systems and Engineering Management

Graduate School of Engineering and Management

Air Force Institute of Technology

Air University

Air Education and Training Command

In Partial Fulfillment of the Requirements for the

Degree of Master of Science in Engineering and Environmental Management

Chris M. Stoppel, B.S.

Captain, USAF

March 2001

AFIT/GEE/ENV/01M-21

A MODEL FOR PALLADIUM CATALYZED DESTRUCTION OF CHLORINATED ETHENE CONTAMINATED GROUNDWATER

Chris M. Stoppel, B.S.
Captain, USAF

Approved:

Dr. Mark N. Goltz Chairman, Advisory Committee	1 Mar 01 date
Dr. Abinash Agrawal Member, Advisory Committee	2/26/01 date
Dr. David R. Burris Member, Advisory Committee	2/26/01 date
Dr. Junqi Huang Member, Advisory Committee	2/26/2001 date

Acknowledgements

There are many individuals whom I'd like to recognize for helping me complete this thesis. First and foremost is my thesis advisor, Dr. Mark Goltz. Without his foresight, guidance, and most of all patience, this thesis would not be anywhere near the product it is now. His engineering insight and ability to explain concepts in such a manner that even I could understand spared me a great deal of time and frustration.

Both my parents and wife's parents provided outstanding support during the past 18 months that deserves recognition. Their witty sense of humor, understanding, and encouragement were extremely helpful. I am extremely blessed to be their son and can only hope to become the man, husband, and father that my own father and father-in-law are today. They are the true role models in my life.

Finally, I want to recognize the one person that contributed the most support to me finishing this thesis. Words cannot describe the appreciation I have for my wife. Her encouragement, support, and most of all love, are a constant reminder of how fortunate I am to enjoy life with her as a life-long companion. This thesis is dedicated to her.

Chris M. Stoppel

Table of Contents

Page

Acknowledgements iv

List of Figures vii

List of Tables ix

Abstract x

1.0 INTRODUCTION 1
1.1 MOTIVATION 1
1.2 RESEARCH OBJECTIVE 5
1.3 RESEARCH APPROACH 6
1.4 SCOPE AND LIMITATIONS OF RESEARCH 6

2.0 LITERATURE REVIEW 9

2.1 INTRODUCTION 9
2.2 Pd/H_2 REACTION MECHANISM 9
2.3 EXPERIMENTAL RESULTS 11
2.3.1 CATALYST SUPPORT 14
2.3.2 HYDROGEN GAS 17
2.3.3 EFFECT OF OTHER CHLORINATED ETHENE CONTAMINANTS ON CATALYTIC REACTION 22
2.3.4 EFFECT OF GROUNDWATER CHEMISTRY ON CATALYTIC REACTION 23
2.3.5 CATALYST REGENERATION 31
2.4 MODELING Pd/H_2 HYDRODEHALOGENATION 32
2.5 FIELD APPLICATIONS 39
2.6 HORIZONTAL FLOW TREATMENT WELLS (HFTWs) 42
2.6.1 FERLAND'S (2000) Pd/H_2 REACTOR SUBMODEL 47

3.0 METHODOLOGY 49

3.1 INTRODUCTION 49
3.2 IN-WELL Pd/H_2 REACTOR SUBMODEL 49
3.2.1 MODEL ASSUMPTIONS 49
3.2.2 MODELING CATALYST DEACTIVATION 52
3.2.3 MODELING REGENERATION 56
3.2.4 SUBMODEL LIMITATIONS 57
3.3 INCORPORATION OF Pd/H_2 SUBMODEL INTO HFTW MODEL 58
3.4 SENSITIVITY ANALYSIS 59
3.5 MODEL VERIFICATION 61

Page

4.0 ANALYSIS 62

4.1 INTRODUCTION 62
4.2 SENSITIVITY ANALYSIS 62
4.2.1 REACTOR SUBMODEL 62
4.3 MODEL PREDICTIONS COMPARED TO EXPERIMENTAL RESULTS 66
4.4 HFTW SYSTEM (2 WELLS) 69
4.4.1 FLOW RATE 70
4.4.2 WELL SEPARATION DISTANCE 72
4.5 GENERAL APPLICATION TO HYPOTHETICAL SITE 75
4.5.1 MODEL COMPARISON 76

5.0 CONCLUSIONS 78

5.1 SUMMARY 78
5.2 CONCLUSIONS 78
5.3 RECOMMENDATIONS 80

BIBLIOGRAPHY 82

VITA 86

List of Figures

Page

Figure 1.1: Schematic of Horizontal Flow Treatment Well (HFTW) System With In-Well Pd Reactors (after Ferland, 2000) 8

Figure 2.1: Proposed Reaction Pathway of TCE to Ethane using Pd/H_2 system (Lowry and Reinhard, 1999) 11

Figure 2.2 Schematic of Pd/H_2 system using in-well catalytic reactors (McNab et al., 2000) 40

Figure 2.3 HFTW operating in two aquifers (after Ferland, 2000) 44

Figure 2.4 Plan view of 2-well HFTW system (upper aquifer shown) 44

Figure 2.5 HFTW efficiency contour plot at $\alpha = 67.5$ deg (after Ferland, 2000) 47

Figure 3.1 Calibrating the submodel to experimental data (Lowry and Reinhard, 2000a) $TCE_{in} = 3.5$ mg/L, $Q = 1$ ml/min, $V = 0.7$ ml, $t_r = 0.3$ min, $g_{cat} = 0.5$ gm 56

Figure 3.2 Submodel output including multiple catalyst regenerations 56

Figure 3.3 Alpha values that equalize interflow for various B_U/B_L and V_{col}/V_{gw} ($A = 0.018$ m^2, $d_{half} = 8$ m) 60

Figure 4.1 Effect of increasing g_{cat} for equal mass contaminant/poison loading 63

Figure 4.2 Effect of increasing residence time on single-pass- efficiency by a) decreasing flow rate (Q) and b) increasing column length (L) 64

Figure 4.3 Effect of injecting additional poison (SO_3^{2-}) on single-pass efficiency ($Q = 1$ mL/min) 65

Figure 4.4 Single-pass efficiency (η_{sp}) as a function of non-dimensional operating time ($T^* k_d$) and non-dimensional residence time ($t_r * k_{obs0}$) 65

Figure 4.5 Magnified view of Figure 4.4 66

Figure 4.6 Submodel output compared to experimental column results (Figure 5b, Lowry and Reinhard (2000a)) 67

Page

Figure 4.7 Submodel output compared to experimental column results using Moffett groundwater (Figure 6a, Lowry and Reinhard (2000a)) 68

Figure 4.8 Effect of increasing pumping rate on HFTW efficiency ($\eta_{overall}$) 71

Figure 4.9 Effect of decreasing the well separation distance on HFTW efficiency 72

Figure 4.10 HFTW efficiency contour plots at T = 5, 10, 15, 20 days (α = 90 deg, $B_U = B_L$ = 8 m, k_d = 0.1 day^{-1}) 74

Figure 4.11 Overall efficiency vs time for HFTW system operation using Table 4.2 parameters 75

Figure 4.12 Comparison of HFTW models 76

List of Tables

Page

Table 2.1 CHC Transformation Rate Constants and Half Lives in Zero-Headspace Reactor Using Pd/Al (Lowry and Reinhard, 1999) 12

Table 2.2 Observed rate constants in batch experiments performed at various aqueous hydrogen concentrations. (Lowry and Reinhard, 2000b) 18

Table 2.3 Effect of nitrite solute on TCE destruction on Pd/Al catalyst 22

Table 2.4 Observed rate constants of simultaneous multiple contaminants destruction performed in batch experiments (Lowry and Reinhard, 2000b) 23

Table 2.5 Common groundwater constituents and their effect on catalyst activity 30

Table 2.6 Deactivation rate constants for various groundwater constituents (Lowry and Reinhard, 2000b) 37

Table 3.1 First-order reaction rate constants for various contaminant/solute concentrations (Lowry and Reinhard, 2000a) 53

Table 3.2 Baseline k_d values and corresponding experimental parameter values 54

Table 3.3 M_{kd} values for TCE and known catalyst poisons 55

Table 4.1 Engineering parameters affecting HFTW treatment efficiency 70

Table 4.2 HFTW operating parameters and regional aquifer characteristics 71

Table 4.3 Parameters affected by pumping rate (Q) and well separation distance (d_{half}) 73

Table 4.4 Hypothetical scenario conditions (taken from Edwards AFB) 76

Abstract

Groundwater contamination by chlorinated ethenes is a widespread environmental problem. Conventional remediation technologies have shortcomings that have prompted further research into the development of novel treatment technologies. A palladium/ alumina catalyst in the presence of dissolved molecular hydrogen (referred to hereafter as a Pd/H_2 system) has been demonstrated to rapidly destroy chlorinated ethene contaminated groundwater. First-order kinetics have been used to model chlorinated ethene destruction in a Pd/H_2 reactor. However, catalyst deactivation and regeneration are important processes that also need to be modeled in order to better understand their effect on treatment efficiency. This study presents a model for palladium catalyzed destruction of chlorinated ethenes that includes catalyst deactivation and regeneration. The model is validated using experimental column results (Lowry and Reinhard, 2000a). The model is then coupled with an analytical groundwater flow model to simulate application of in-well Pd/H_2 reactors to treat chlorinated ethene contaminated groundwater in a recirculating Horizontal Flow Treatment Well (HFTW) system. Applying the model under realistic conditions results in approximately 130 days of HFTW system operation without significant catalyst deactivation. This suggests catalyst deactivation will not significantly affect operating costs or system performance in a real remediation scenario. The model presented in this study, by incorporating the relevant processes of catalyst deactivation and regeneration, represents an important step in transitioning the Pd/H_2 in-well system toward field application.

A MODEL FOR PALLADIUM CATALYZED DESTRUCTION OF CHLORINATED ETHENE CONTAMINATED GROUNDWATER

1.0 INTRODUCTION

1.1 MOTIVATION

Groundwater contamination by chlorinated ethenes, such as tetrachloroethene (PCE) and trichloroethene (TCE), is a widespread environmental problem. According to the Agency for Toxic Substances and Disease Registry, TCE and PCE are, respectively, the first and third most commonly detected contaminants at the approximately 330,000 hazardous waste sites across the nation (National Research Council (NRC), 1994). This nationwide problem also affects the Air Force, which is responsible for managing 6,038 hazardous waste sites (Defense Environmental Restoration Program (DERP), 1998). It is estimated that groundwater contamination by chlorinated ethenes is found at over 70 percent of Air Force installations (Ferland, 2000).

PCE and TCE are probable carcinogens that can degrade into vinyl chloride (VC), a known human carcinogen (Vogel and McCarty, 1985; Masters, 1997). As a result, extensive research has been dedicated to developing new technologies that can remediate chlorinated ethene-contaminated groundwater. Three remediation strategies commonly used today to contain chlorinated ethene-contaminated groundwater are pump-and-treat systems, permeable reactive barrier systems, and natural attenuation. Unfortunately, all three strategies have shortcomings that will now be discussed in depth.

Pump-and-treat systems pump water from contaminated aquifers to aboveground treatment facilities for remediation. The treated effluent can then be used, discharged to surface water, or returned to the aquifer (Masters, 1997). In 1997, pump-and-treat systems were in operation at nearly three-quarters of all groundwater remediation projects (Masters, 1997). One disadvantage of pump-and-treat is that frequently, the aboveground treatment process does not destroy the contaminants, but simply transfers them to another medium like air (during air stripping) or Granular Activated Carbon (GAC). Another disadvantage is the increased cost and risk of exposure resulting from pumping contaminated groundwater to the surface. In a study of 77 contaminated sites, the Committee on Ground Water Cleanup Alternatives for the National Research Council in 1994 concluded that pump and treat would be the optimal choice for only a limited range of circumstances to achieve cleanup goals at reasonable costs (Masters, 1997).

Permeable reactive barriers (PRBs) typically employ low hydraulic conductivity "funnels" that channel the flow of contaminated groundwater through a treatment "gate" or reactive barrier (Starr and Cherry, 1994). Research by Hannesin and Gillham (1998), and McMahon et al. (1999) has shown that zero-valent iron installed as a reactive barrier can successfully dehalogenate chlorinated ethenes at relatively low operational costs. One problem with using zero-valent iron is the potential of clogging due to precipitation or biological growth (McMahon et al., 1999; Gu et al. 1999). Additionally, PRBs can only be used for a limited range of hydrogeological conditions. The barriers can only be installed at a limited depth, and changes in groundwater flow could allow the contaminant plume to bypass the PRB.

Under proper conditions, microbially mediated dehalogenation can result in natural attenuation of chlorinated ethenes that is protective of human health and the environment. Natural attenuation uses physical, chemical, and biological processes inherent to the contaminated subsurface to effectively destroy unwanted compounds to achieve remediation objectives in a reasonable period of time. The EPA defines monitored natural attenuation as:

> ...the reliance on natural attenuation processes (within the context of a carefully controlled and monitored clean-up approach) to achieve site-specific remedial objectives within a time frame that is reasonable...[They] include a variety of physical, chemical, or biological processes that...act without human intervention to reduce mass, toxicity, mobility, volume, or concentration of contaminants in soil and groundwater (US EPA, 1997).

The Office of Solid Waste and Emergency Response (OSWER) acknowledges the existence of potential mechanisms for biodegradation of chlorinated solvents, but also states that "the hydrogeologic and geochemical conditions favoring significant biodegradation of chlorinated solvents sufficient to achieve remediation objectives within a reasonable timeframe are anticipated to occur only in limited circumstances" (OSWER Directive 9200.4-17P, 1999). Therefore, until our understanding of these natural occurring processes is increased, monitored natural attenuation will continue to have limited use for the management of chlorinated solvents. Another disadvantage of natural attenuation is that the natural processes may take too long to be protective of human health and the environment. A third disadvantage is the public's view of this strategy as "doing nothing," though a better understanding of the processes associated with this strategy may reduce the public's skepticism.

As a result of the shortcomings in the aforementioned remediation strategies, innovative technologies are needed to improve remediation efficiency, expediency, and cost. Recent laboratory experiments and field studies (Lowry and Reinhard, 2000a; McNab et al., 2000) have shown rapid destruction of chlorinated ethenes using a palladium catalyst with hydrogen gas. One innovative technology proposed by Ferland (2000) consists of a Horizontal Flow Treatment Well (HFTW) system with an in-well Palladium catalytic reactor utilizing injected dissolved hydrogen gas (see Figure 1.1). HFTWs have been used successfully in the past. McCarty et al. (1998) used an HFTW system to create and maintain bioactive zones by injection of toluene, oxygen, and hydrogen peroxide to treat TCE-contaminated groundwater at Site 19, Edwards Air Force Base, CA. Total TCE removal efficiencies were 97 – 98% (McCarty et al., 1998). These high efficiencies were due in part to the design of the HFTW system, which allowed for multiple passes of contaminated groundwater through the bioactive zones. In the HFTW system, some wells pump in an upward mode, while other wells pump in a downward mode. This bi-directional flow creates a recirculating flow pattern between the wells, as shown in Figure 1.1, which in turn allows the contaminant to make multiple passes through the treatment system, thereby increasing contaminant removal efficiency (Ferland, 2000). HFTWs possess the advantages of both pump-and-treat and PRB remediation strategies. It is an active technology (like pump-and-treat) that allows control of plume migration, thereby reducing the chance of the contaminant bypassing the remediation system, as might occur with a passive technology like PRBs. Like PRBs however, the treatment is in situ; therefore the costs and health risks associated with pumping contaminated water to the surface are greatly reduced.

In order for this in situ treatment to be effective, the in-well reactor must have a very fast reaction time. Based on the laboratory work of Lowry and Reinhard (2000) and the modeling work of Ferland (2000), it appears a Palladium catalyst with hydrogen gas (Pd/H_2) may be effective for in-well use in an HFTW system. Ferland (2000) used first-order kinetics to model chlorinated-ethene destruction in the reactor. However, long-term experiments have indicated catalyst degeneration with time (McNab et al., 2000). There is also a concern that common groundwater constituents like sulfur species (HS^- or SO_3^{2-}) and the accumulation of organic or biological dendritic structures on the catalyst surface contribute to catalyst deactivation (Lowry and Reinhard, 2000a; Munakata et al., 2000).

1.2 RESEARCH OBJECTIVE

This thesis research will develop and implement a model to increase our understanding of how an HFTW system with in-well Pd/H_2 catalysts can be used to remediate chlorinated ethene contaminated groundwater. The model will then be incorporated into Ferland's (2000) remediation model to simulate field-implementation of this technology. The performance predictions of Ferland's (2000) model will be compared to the predictions of the more complex model developed in this study. This model will serve as a valuable tool in design and field implementation of HFTW systems with Pd/H_2 in-well reactors.

Specific questions will focus on hypothesized mechanisms for the destruction of chlorinated-ethenes using the Pd/H_2 catalyst, the potential effects of natural groundwater constituents on catalyst activity, possible measures to prevent catalyst deactivation and

determination of the relevant processes that influence catalyst effectiveness and longevity.

1.3 RESEARCH APPROACH

(1) Determine what mechanisms are relevant to the dehalogenation of chlorinated-ethenes using a Pd/H_2 reactor and what processes (poisoning, long-term deactivation, etc.) may interfere with the dehalogenation rate and extent.

(2) Determine what measures might be taken to optimize the Pd/H_2 reactor performance.

(3) Develop a model that describes the dehalogenation of chlorinated-ethene contaminants using a Pd/H_2 reactor. The model will take into account processes that have been observed in long-term experiments, such as catalyst deactivation, and regeneration.

(4) Incorporate the Pd/H_2 reactor model as a submodel to simulate an in-well reactor in an HFTW system used to contain chlorinated-ethene contaminated groundwater.

1.4 SCOPE AND LIMITATIONS OF RESEARCH

(1) Research will only consider a Pd/H_2 reactor for use as the in-well catalytic reactor in an HFTW system. Other potential reactors will not be studied.

(2) The model will be developed based on review of the literature and recent experimental results from studies at Wright State University. This study will not include independent laboratory experimentation.

(3) The model will only consider the destruction of chlorinated ethenes in contaminated groundwater. Other contaminants that may be destroyed by a Pd/H_2 reactor will not be considered.

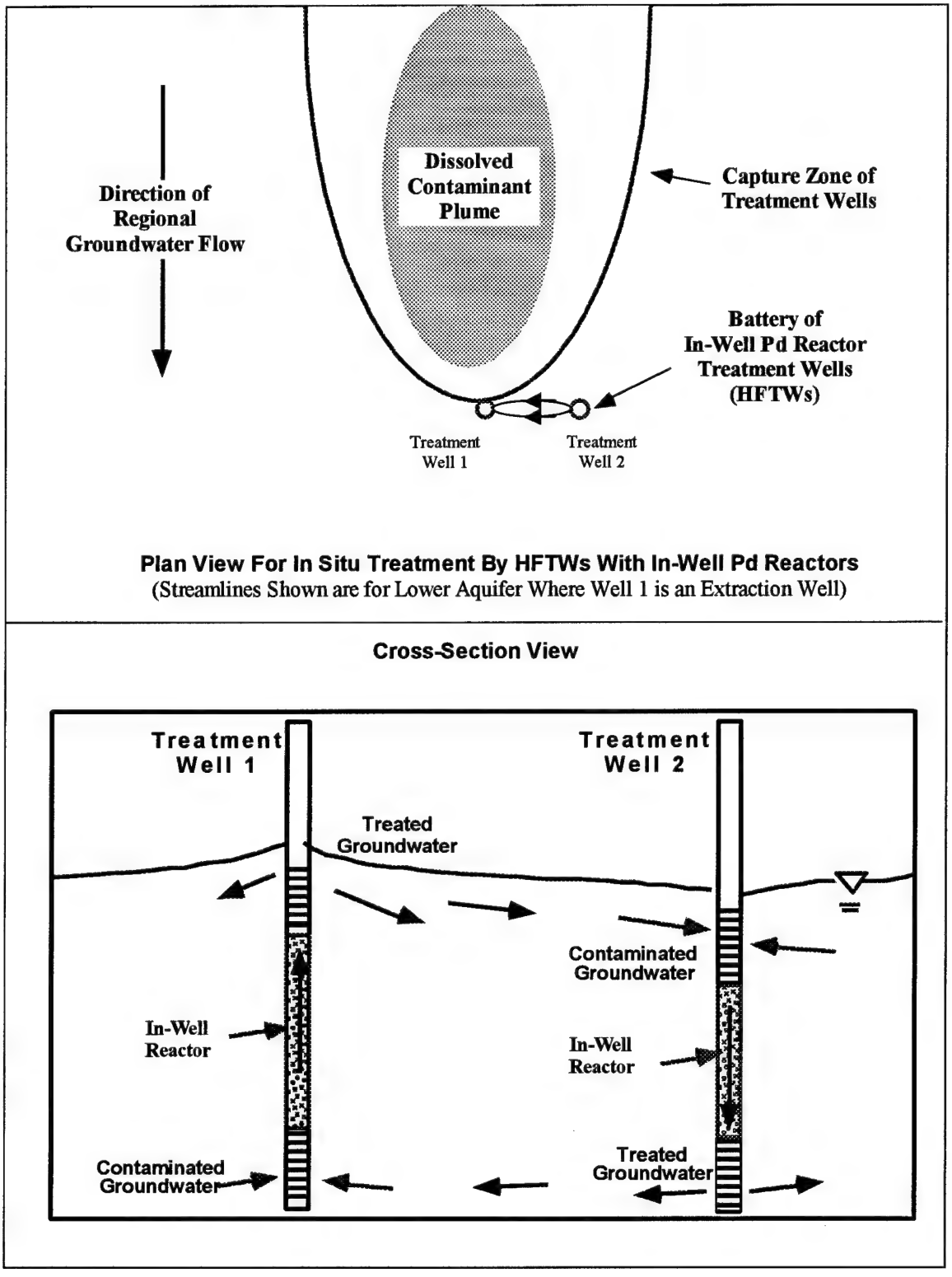

Figure 1.1: Schematic of Horizontal Flow Treatment Well (HFTW) System With In-Well Pd Reactors (after Ferland, 2000)

2.0 LITERATURE REVIEW

2.1 INTRODUCTION

This chapter summarizes the literature pertinent to the destruction of chlorinated ethenes in a Pd/H_2 system. It reviews the laboratory and modeling studies that have been conducted to gain understanding into the rate, extent, and mechanisms of this hydrodehalogenation process. This chapter will also review modeling studies and field applications of HFTW systems and how this technology combined with the Pd/H_2 system is envisioned to effectively destroy chlorinated ethenes.

2.2 Pd/H_2 REACTION MECHANISM

Research devoted to catalytic hydrodehalogenation can be traced back to the early 1950's (Rylander, 1979). While this method was widely used in chemical synthesis, the technology was not introduced to groundwater remediation until the early 1990s (Kovenklioglu et al., 1992). Hydrodehalogenation is a process of hydrogenation (adding hydrogen ions) and dehalogenation (removing halide ions). This is accomplished by way of noble metals, like palladium, in the presence of hydrogen gas. Upon contact with the metal, hydrogen gas disassociates into hydrogen ions and electrons (Thomas, 1997):

$$H_2 \xrightarrow{Pd} 2H^+ + 2e^-$$

Hydrogen ions replace halogen ions of chlorinated ethene molecules bound to the catalyst to complete this reaction. Hydrogen gas is oxidized and the contaminant is reduced to harmless daughter products, like ethene and ethane (Lowry and Reinhard, 2000a).

The addition of hydrogen gas to the system has the additional advantage of displacing dissolved oxygen (McNab et al., 2000). While dissolved oxygen is not a catalyst poison, it can reduce dechlorination rates by competing for active sites on the catalyst (McNab et al., 2000). Compounds that may poison the catalyst are discussed later in Section 2.3 and 2.6.

An advantage of the Pd/H_2 system is its ability to reduce chlorinated ethenes directly to ethane at the catalyst surface (Lowry and Reinhard, 1999). This is significant, as the potential for production of chlorinated intermediate products like vinyl chloride is considerably reduced. Lowry and Reinhard (1999) performed batch experiments using metallic palladium (Pd-met) and palladium supported on an alumina catalyst (Pd/Al_2O_3, hereafter referred to as 'Pd/Al') to reductively dehalogenate TCE. While using Pd-met, 3 – 4% of the original TCE concentration was detected as chlorinated intermediates. However, Pd/Al reduced TCE to ethane with no detection of chlorinated daughter products (Lowry and Reinhard, 1999). Based on their findings, Lowry and Reinhard (1999) proposed the pathways shown in Figure 2.1 for TCE transformation to ethane. Based upon the lack of chlorinated intermediates and the stoichiometric production of ethane, Lowry and Reinhard (1999) hypothesized that TCE is largely converted directly to ethane at the catalyst surface (i.e. majority of TCE is transformed to ethane via k_9). It is suspected that the alumina support plays a vital role in facilitating this direct transformation as will be explained in Section 2.3.1.

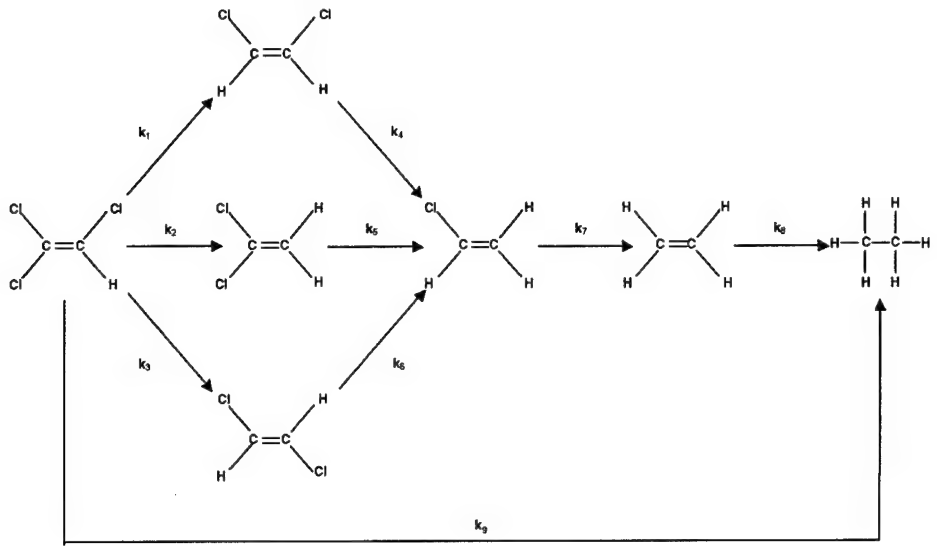

Figure 2.1: Proposed Reaction Pathway of TCE to Ethane using Pd/H_2 system (Lowry and Reinhard, 1999)

2.3 EXPERIMENTAL RESULTS

Laboratory experiments represent a vital step toward developing a new technology. These experiments allow us to gain a better understanding of the technology, as well as helping us learn under controlled conditions how varying individual operating parameters affects technology performance. In this section, we briefly summarize the results of various laboratory experiments that focus on application of the Pd/H_2 system to treat chlorinated ethene – contaminated groundwater. While some of the initial work reported in this section involves catalysts other than Pd, all the studies used H_2 gas as the sole electron donor.

Kovenklioglu et al. (1992) were one of the first researchers to investigate the potential of a Pd/H_2 system for remediating chlorinated hydrocarbon (CHC) contaminated groundwater (Kovenklioglu et al., 1992). Shaker reactors (500 mL) were used to determine the best metallic catalyst among three candidates: palladium, platinum and

rhodium (Kovenklioglu et al., 1992). Of the three metals tested, palladium exhibited the highest activity, as had been expected based upon prior studies (Kovenklioglu et al., 1992; Rylander, 1979).

Lowry and Reinhard (1999) tested 12 CHCs (including PCE, TCE, and the three DCE isomers) to determine the Pd catalyst's effectiveness over a wide range of potential groundwater contaminants. Batch experiments with and without headspace were performed in these studies. Headspace reactors were used to determine rate constants along specific pathways and intermediate product distribution, while zero-headspace reactors were used to determine reaction rate constants and substrate half-lives.

Results of Lowry and Reinhard's (1999) zero-headspace reactor experiments are shown in Table 2.1. The normalized first-order reaction rate constant (k_{rxn}) is obtained by dividing the observed first-order rate constant (k_{obs}) by the catalyst concentration (0.22 g_{cat}/L). For a fuller discussion of rate constants, see Section 2.4. The observation that $k_{PCE} < k_{TCE} < k_{DCE}$ contradicts expected reaction rate values based on bond disassociation energies (Lowry and Reinhard, 1999). Reasons for this trend are still unknown at this time.

Reactant	$[C]_0$ (μM)	k_{rxn} ($L\ g_{cat}^{-1} min^{-1}$)	$t_{1/2}$ (min)
PCE	7.8	0.53	5.9
TCE	22.8	0.64	4.9
1,1-DCE	23.7	0.70	4.5
cis-DCE	76.3	0.83	3.8
trans-DCE	75.3	0.78	4.0

Table 2.1 CHC Transformation Rate Constants and Half Lives in Zero-Headspace Reactor Using Pd/Al (Lowry and Reinhard, 1999)

Lowry and Reinhard (2000a) later performed column experiments with DI water, TCE, and a relatively small amount of Pd/Al (0.5 g) catalyst to provide maximum sensitivity to change in catalyst activity. TCE conversion rapidly declined from 45% - 32 % within the first 2 – 3 days of operation. Following this sharp decline in catalyst activity, catalyst deactivation was still observed, but at a lesser rate. This brief period of rapid deactivation is most likely due to microscale changes in the catalyst surface and is common in most heterogeneous catalytic systems (Thomas, 1997). Lowry and Reinhard (2000a) deemed this transient phenomenon irrelevant to investigating long-term system performance and it was not further investigated.

While the relatively fast reaction rates and small half-lives shown in Table 2.1 are perhaps attributable to the palladium's high activity, the catalyst support and reaction with hydrogen gas are two additional factors that contribute to the effectiveness of the Pd/H_2 system and are discussed in greater detail in the next two sections. We will also discuss the effect of groundwater chemistry upon the catalytic reaction.

Before proceeding any further, let us define two ways in which the efficiency of the Pd/H_2 system decreases. First, solutes in the groundwater may react with aqueous hydrogen gas, thereby reducing the amount of hydrogen available for chlorinated ethene destruction. This process is more commonly referred to as catalyst inhibition, since the catalyst's ability to destroy chlorinated ethenes is inhibited by the reduced amount of aqueous hydrogen. No physical damage is done to the catalyst. The second process that lowers system efficiency is catalyst deactivation, whereby organic or inorganic

compounds absorb to the catalyst surface, effectively reducing the number of active sites for contaminant destruction.

2.3.1 CATALYST SUPPORT

The catalyst support plays an important role in determining catalyst effectiveness by its ability to adsorb target compounds to the catalyst surface. Various supports for palladium, such as alumina (Pd/Al) and carbon (Pd/C), as well as unsupported metallic palladium (Pd-met) have been tested to optimize the catalyst's ability to dehalogenate (Kovenklioglu et al., 1992; Schreier and Reinhard, 1995; Lowry and Reinhard, 1999.) Of Pd/Al, Pd/C, and Pd-met, Pd/Al has demonstrated the greatest success over a wide range of CHCs (Schreier and Reinhard, 1995; Lowry and Reinhard, 1999).

Kovenklioglu et al. (1992) selected carbon as the catalyst support due to its ability to adsorb CHC's to the catalyst surface. Various carbon supports were compared using 1,1,2-trichloroethane (1,1,2-TCA); TCE; chloroform (CF); carbon tetrachloride (CTET); 1,2,4-trichlorobenzene; and dichloromethane as target compounds (Kovenklioglu et al., 1992). An alumina support was also tested with 1,1,2-TCA as the target compound. However, it was observed that 1,1,2-TCA did not degrade. The Pd/Al catalyst's inability to dechlorinate TCA is documented in other sources as well (McNab and Ruiz, 1998; Lowry and Reinhard, 2000a).

Schreier and Reinhard (1995) also compared the alumina and carbon supports by examining their ability to destroy various chlorinated ethenes (PCE, TCE, cis-

dichloroethene (cis-DCE), trans-DCE, and VC). Experiments were performed in a 125 mL glass bottle containing 60 mL tap water, 1.0 μmol of substrate (chlorinated ethene), and either 0.5 g of 0.5% Pd/Al (0.5% Pd by weight) or 1% Pd/C (1% Pd by weight) (Schreier and Reinhard, 1995). Hydrogen was added to the system via syringe, while an orbital shaker accomplished complete mixing of constituents (Schreier and Reinhard, 1995). The alumina support exhibited an 85% ethane yield from the original PCE concentration. The ethane yield serves as an indicator of dechlorination occurring at the catalyst surface (i.e. the greater the ethane yield, the greater the CHC conversion at the catalyst surface). The Pd/Al catalyst showed slightly lower ethane yields for the remaining chlorinated ethenes (70% – 75%) with the exception of trans-DCE, which had a significantly lower yield (55%). PCE destruction was observed to a lesser extent using the Pd/C catalyst (55% ethane yield) (Schreier and Reinhard, 1995). It's speculated that this lower ethane yield is due to side reactions occurring on the catalyst surface due to the presence of the carbon support (Schreier and Reinhard, 1995). It is also interesting to note that while the carbon support had a greater amount of palladium than the alumina support (1% vs 0.5%), a far lower ethane yield was achieved. Higher ethane yields exhibited by the alumina support demonstrate destruction of CHC from groundwater and not a mere transfer from groundwater to another media (carbon support).

Lowry and Reinhard (1999) performed batch experiments in headspace reactors to compare Pd-met and Pd/Al at TCE initial concentrations of 250 μM and 25.3 μM, respectively. No chlorinated intermediates were detected using the Pd/Al catalyst while approximately 3% - 4% of the original TCE was detected as chlorinated intermediates at

their respective maximum concentrations. It is speculated that the alumina support adsorbs chlorinated intermediates, thus aiding to suppress their detection in water (Lowry and Reinhard, 1999). It is interesting to note that Lowry and Reinhard (2000b) detected chlorinated intermediates when this same experiment was repeated at a higher TCE initial concentration (160 μM) and various aqueous hydrogen gas concentrations. Approximately 3% of the total TCE transformed were detected as chlorinated intermediates under high aqueous hydrogen concentration (1000 μM) (Lowry and Reinhard, 2000b). While it is likely that the lack of chlorinated intermediates detected in Lowry and Reinhard's 1999 batch experiments is partially due to adsorption of these intermediates to the catalyst surface, it is also likely that a small fraction of these intermediates desorbed from the catalyst, yet small enough to elude detection. As a TCE molecule is adsorbed to the catalyst surface, one, two, or three chlorine atoms may be replaced by hydrogen before desorbing from the catalyst. However, the preferred pathway is a direct transformation to a non-chlorinated constituent as indicated by the relatively small percentage of detected chlorinated intermediates (Lowry and Reinhard, 1999 and 2000b).

TCE reduction experiments in the headspace reactor were performed separately with Pd/Al and Pd-met. No chlorinated intermediates were detected using the Pd/Al catalyst while 3% - 4% of original TCE was detected as DCE or VC using the Pd-met catalyst. This lends support to the hypothesis that the alumina support adsorbs intermediate products, thereby suppressing their detection (Lowry and Reinhard, 1999). Intermediate and final product distributions were determined by carbon mass balance. While the

Pd/Al experiment showed nearly complete dehalogenation to ethane (97%) and ethene (<1%), the Pd-met experiment yielded ethane (83%) and two unidentified compounds (Lowry and Reinhard, 1999).

2.3.2 HYDROGEN GAS

Hydrogen gas (H_2) plays a crucial role in the effectiveness of this remediation technology by donating electrons to reduce the chlorinated ethenes. Past experimental work has tested the Pd/H_2 system at or near hydrogen saturated water conditions (Munakata et al., 1998; Lowry and Reinhard, 1999; McNab et al., 2000). Until recently however, no research has been conducted to evaluate the effects of limited aqueous hydrogen concentrations ($[H_2]_{(aq)}$) on the destruction of chlorinated ethenes from contaminated groundwater. Lowry and Reinhard (2000b) performed batch and column experiments with Pd/Al and TCE at various aqueous hydrogen concentrations to determine the effect on contaminant removal efficiency, intermediate and final product distribution, catalyst deactivation due to production of radical coupling products, and the effects from hydrogen-utilizing competing solutes.

Lowry and Reinhard (2000b) performed batch experiments to evaluate TCE transformation rates at various aqueous hydrogen concentrations. The batch reactor was purged with H_2:N_2 gas at various pre-determined ratios to establish known aqueous hydrogen concentrations and to displace any remaining dissolved oxygen (Lowry and Reinhard, 2000b). Only a small amount of powdered Pd/Al (0.1g) was used, so that

small variations in catalyst activity could be detected. Table 2.2 lists the observed first-order rate constants (k_{obs}) at various aqueous hydrogen gas concentrations.

$[H_2]_{(aq)}$ (μM)	k_{obs} $(min^{-1})^1$
1000	0.034 ± 0.006
400	0.025 ± 0.004
100	0.015 ± 0.001
40	0.0037 ± 0.0005
10	0.0007 ± 0.0003

[1]- figures represent 95% confidence intervals

Table 2.2 Observed rate constants in batch experiments performed at various aqueous hydrogen concentrations. (Lowry and Reinhard, 2000b)

In addition to decreasing the observed rate constant, decreasing the aqueous hydrogen concentration increased the production of chlorinated intermediates. While only 3% of the total TCE transformed was converted to chlorinated daughter products under hydrogen-rich conditions ($[H_2]_{(aq)}$= 1000 μM), chlorinated daughter products increased to 9.8% of the total TCE transformed under hydrogen-limiting conditions ($[H_2]_{(aq)}$= 10 μM) (Lowry and Reinhard, 2000b). Based on less chlorinated daughter products appearing and then disappearing in batch experiments, and the lack of detection of these chlorinated intermediates in column experiments, it appears that the formation of chlorinated intermediates is a transient process (Lowry and Reinhard, 2000b). However, the rates at which these intermediates are produced and subsequently destroyed are dependent on the aqueous hydrogen concentration. Higher aqueous hydrogen concentrations increased both the production and destruction rates of these intermediates (Lowry and Reinhard, 2000b).

It is interesting to note that while intermediate production increased with decreasing aqueous hydrogen gas concentration, the distribution among intermediate products was relatively constant, indicating that the aqueous hydrogen concentration has little effect on intermediate product distribution (Lowry and Reinhard, 2000b). The product distribution at the maximum intermediate product concentration was (in descending order): cis-DCE, 1,1-DCE, trans-DCE, and VC. This product distribution is consistent with the results of Lowry and Reinhard's (1999) batch experiment using a Pd-met catalyst.

Although ethene is the primary product in the destruction of chlorinated ethenes, C4 and C6 radical couple products were also detected in batch experiments performed by Lowry and Reinhard (2000b). Radical couple production comprised approximately 1% of total TCE transformed under hydrogen-rich conditions (1000 μM), and increased to 18% upon lowering the aqueous hydrogen concentration to 10 μM. N-butane is the most abundantly produced radical couple product at aqueous hydrogen concentrations greater than 100 μM, but the production shifts towards unsaturated radical couples (1-butene, cis-2-butene, trans-2-butene, and 2-hexene) at aqueous hydrogen concentrations below 100 μM. It is speculated that catalyst deactivation at lower aqueous hydrogen concentrations (<100 μM) may partially be due to adsorption of these unsaturated radical couples on the catalyst surface, thereby reducing the effective catalyst area for catalyzed destruction of (Lowry and Reinhard, 2000b). C4 and C6 radical couple products were not detected in column experiments, but only in batch experiments.

2.3.2.1 COMPETITION FOR H_2

Other solutes in the groundwater may react with aqueous hydrogen gas, thereby reducing the amount of hydrogen available for chlorinated ethene destruction. Oxygen is an important competitor for H_2, as it reacts with hydrogen to form water at the catalyst surface, as seen in the following reaction (Lowry and Reinhard, 2000b).

$$2H_2 + O_2 \xrightarrow{Pd} 2H_2O$$

Lowry and Reinhard (2000b) performed column experiments at various dissolved oxygen and aqueous hydrogen concentrations to determine the effect of dissolved oxygen on contaminant removal efficiency in the Pd/H_2 system. Although hydrogen reacted more rapidly with oxygen than it reacted with TCE, dissolved oxygen concentrations below 370 μM (11.8 mg/L) did not adversely impact TCE destruction so long as aqueous hydrogen concentrations were in the range 670 - 790 μM (Lowry and Reinhard, 2000b). TCE conversion dropped significantly at increased influent dissolved oxygen concentrations of 450μM (14.4 mg/L) and 600 μM (19.2 mg/L) and decreased aqueous hydrogen concentrations (550 μM and 420 μM, respectively). Increasing the aqueous hydrogen concentration to 1150 μM permitted unimpaired TCE destruction, even at dissolved oxygen concentrations greater than 11.8 mg/L (17.3 mg/L was the greatest dissolved oxygen concentration tested under hydrogen-saturated conditions). These conclusions support the notion that removal of dissolved oxygen may not be necessary for successful field operation.

Nitrate and nitrite have also been found to react with hydrogen to form nitrogen gas (N_2) according to the following reactions (Lowry and Reinhard, 2000b):

$$2NO_3^- + 5H_2 \xrightarrow{Pd/Cu} N_2 + 2OH^- + 4H_2O$$

$$2NO_2^- + 3H_2 \xrightarrow{Pd} N_2 + 2H_2O + 2OH^-$$

Column experiments at two nitrate concentrations (371 μM and 1290 μM) resulted in no change in TCE destruction and only a slight change in nitrate concentration. Small changes between influent/effluent nitrate concentrations during the first days of the experiment are likely due to adsorption of nitrate to the catalyst surface rather than reaction with hydrogen. The lack of chlorinated intermediates detected in the column effluent supports the notion that nitrate adsorption to the catalyst surface is minimal and does not adversely impact catalyst activity. The non-reactive behavior of nitrate in the column is consistent with past literature stating a bimetallic catalyst is necessary for nitrate to be reactive (Daub et al., 1999; Pintar et al., 1996), though the finding that nitrate does not significantly contribute to catalyst deactivation conflicts with results from Munakata et al. (1998), presented later in Section 2.3.4.

Column experiments were performed with nitrite concentration two orders of magnitude greater than TCE concentration. Nitrite concentrations ranged from 1565 μM (23 mg/L) to 6630 μM (80 mg/L) (Lowry and Reinhard, 2000b). As expected from past work, nitrite was more reactive than nitrate on the Pd catalyst (Daub et al., 1999). An increase in pH from 8.8 to 10.2 due to production of hydroxide ions was observed, along with a drop in nitrite concentration across the catalyst column. Table 2.3 illustrates the effect of high nitrite concentrations on TCE destruction efficiency.

Solute	$[Solute]_{in}$ (μM)	$[TCE]_{in}$ (μM)	TCE Conv (%)	Solute Conv (%)
none	0	26.6	48.2	0
nitrite	1565	23.1	44.0	23
"	2609	30.3	43.3	10
"	6630	25.1	44.4	–

Table 2.3 Effect of nitrite solute on TCE destruction on Pd/Al catalyst
(Copied from Table 4, Lowry and Reinhard, 2000b) (last entry in "Solute Conv" column presumably undetectable)

As seen in Table 2.3, nitrite conversion decreases as its concentration increases, but the decrease in TCE conversion is minimal. This suggests that nitrite conversion is limited and that the presence of nitrite, even at relatively high concentrations, does not significantly impact TCE conversion. Therefore, it is unlikely that nitrite (which typically occurs at relatively low concentrations in groundwater (Lowry and Reinhard, 2000b)) will negatively impact the efficiency of the Pd/H_2 system.

2.3.3 EFFECT OF OTHER CHLORINATED ETHENE CONTAMINANTS ON CATALYTIC REACTION

Many times contaminated groundwater contains more than one contaminant. Lowry and Reinhard (2000b) conducted batch experiments with multiple (TCE, cis-DCE, trans-DCE, and 1,1-DCE) to observe the effects of multiple contaminants on the performance of the Pd/H_2 system. The observed TCE degradation rate constant did not change with respect to previous batch experiments performed with TCE as the sole contaminant. This supports the notion that TCE does not compete with chlorinated intermediates for active catalyst sites (Lowry and Reinhard, 2000b). Table 2.4 summarizes Lowry and Reinhard's (2000b) findings from this experiment.

CHC	[CHC] (μM)	k_{CHC} $(min)^{-1}$
TCE	66	0.04 ± 0.006
cis-DCE	202	0.042 ± 0.003
trans-DCE	89	0.052 ± 0.002
1,1-DCE	91	0.050 ± 0.004

Table 2.4 Observed rate constants of simultaneous multiple contaminants destruction performed in batch experiments (Lowry and Reinhard, 2000b)

The finding that observed rate constants increase with decreasing degree of chlorination ($k_{DCE} > k_{TCE}$) agrees with past experimental results (Lowry and Reinhard, 1999).

2.3.4 EFFECT OF GROUNDWATER CHEMISTRY ON CATALYTIC REACTION

In this section, research conducted to evaluate the potential problems that common groundwater constituents may cause on Pd/H_2 system performance in the field is summarized. Understanding the interactions between naturally occurring groundwater constituents and the Pd/Al catalyst allows us to optimize system performance and avoid premature performance degradation.

Schreier and Reinhard (1995) studied the effects of various groundwater constituents on catalyst performance to determine suitability for field application. Dissolved oxygen was observed to lower catalyst performance by competing with substrate (target contaminant) for hydrogen; however, increasing the system hydrogen pressure minimized this effect (Schreier and Reinhard, 1995). Nitrite, nitrate, and sulfate were also investigated as potential catalyst inhibitors (Schreier and Reinhard, 1995). The concentration of each ion added to solution was an order of magnitude greater than the target contaminant concentration (PCE) (Schreier and Reinhard, 1995). Although all three ions adversely

affected catalyst efficiency, nitrite had the greatest effect on catalyst inhibition, reducing dechlorination by 50% (Schreier and Reinhard, 1995).

Munakata et al. (1998) also examined potential effects on catalyst effectiveness in a Pd/H_2 system due to various groundwater constituents by performing bench-scale column experiments in a variety of groundwater matrices. Hydrogen saturated water was mixed with TCE prior to being injected into a column containing the catalyst (Munakata et al., 1998). The following water matrices were used in the study: deionized (DI) water; DI water spiked with nitrate, phosphate, carbonate (in the form of Na_2CO_3), and carbon dioxide; and groundwater from Lawrence Livermore National Laboratory (LLNL) (Munakata et al., 1998).

Munakata et al.'s (1998) baseline column experiments using deionized water resulted in sustained TCE removal efficiencies of > 99% over five months. Introducing 44 mg/L nitrate into the column decreased catalyst efficiency to 52% (Munakata et al., 1998). Discontinuing the nitrate addition resulted in the catalyst returning to original efficiency levels, supporting the hypothesis that nitrate competes with TCE for hydrogen and active catalyst sites (Munakata et al., 1998). High phosphate concentrations (100 mg/L) produced minor but significant losses of catalyst efficiency (Munakata et al. 1998). The most notable catalyst deactivation resulted from the carbonate (Na_2CO_3)- and carbon dioxide- amended DI water. Catalyst efficiency was reduced to 17.5% after 5.5 days inflow of Na_2CO_3 amended DI water; while complete catalyst deactivation was observed in CO_2 amended DI water after 13 days (Munakata et al., 1998). Catalyst deactivation

was also more rapid in CO_2 amended LLNL groundwater than in LLNL groundwater alone (Munakata et al., 1998). Catalyst regeneration was performed in these experiments and is described in Section 2.3.5.

Using atomic absorption spectrophotometry, trace amounts of dissolved palladium were measured when TCE was present in the DI water, but not in the DI water alone (Munakata et al. 1998). Pd dissolution may be due to low pH regions caused by dehalogenation reactions at the catalyst surface (Munakata et al., 1998). Significant catalyst dissolution was observed in batch experiments at pH < 4.0 (Munakata et al., 1998).

Munakata (2000) further investigated changes at the catalyst surface spectroscopically using XPS analysis. The analysis resulted in identifying biogrowth on the catalyst surface, as indicated by the detection of carbon and nitrogen. In addition to biogrowth, sulfur was detected on the catalyst surface as a result of either sulfate amended DI water or groundwater. The sulfur proved to be weakly sorbed to the catalyst surface as it was removed by washing the catalyst with DI water (Munakata, personal communication). Calcium, however, also sorbed to the catalyst surface and was not removable by washing (Munakata, 2000). Due to the rough and curved edges of the catalyst and small amounts of Pd on the catalyst support, spectroscopic analysis is difficult. In an effort to increase the clarity of the spectroscopic analysis of the dispersed catalyst, Munakata developed a model catalyst consisting of a conductive flat plat, coated with a thin film of Pd. The model catalyst has been determined to be catalytically active in batch experiments and

spectroscopic results coincide with the dispersed catalyst. Efforts to develop a model catalyst for column experiments are on going (Munakata, 2000).

Lowry and Reinhard (2000a) conducted column experiments to investigate the performance of the Pd/Al catalyst in the presence of carbonate and sulfur containing species, which have been suspected catalyst inhibitors (McNab and Ruiz, 1998; Schüth et al. 1998). Catalyst regeneration studies were also performed and discussed in Section 2.3.5. The experimental system was set up so that TCE conversion would be relatively low, in order to better observe catalyst deactivation. This was achieved by using a relatively small amount of Pd/Al catalyst (0.5 g). The catalyst deactivation rate constant in deionized water was used as a baseline to compare with deactivation rate constants from subsequent experiments (Lowry and Reinhard, 2000a). The method for determining the catalyst deactivation rate constant is explained in Section 2.4.

Carbonate (CO_3^-) and carbonic acid (H_2CO_3) were introduced into the column at concentrations an order of a magnitude greater than TCE (Lowry and Reinhard, 2000a). Comparison with the baseline deactivation rate constant indicated no additional catalyst deactivation due to the presence of the carbonate species. This finding somewhat contradicts Munakata et al.'s (1998) experimental results involving catalyst deactivation with Na_2CO_3-amended DI water. While catalyst deactivation was not attributable to the presence of carbonate species, the change in pH due to the presence of a particular carbonate species may have had a minor effect upon catalyst efficiency. Degradation rate constants were observed to be greater in the presence of carbonate (pH = 11.0) than in the

presence of carbonic acid (pH = 4.3) (Lowry and Reinhard, 2000a). This is consistent with prior catalyst studies that showed high pH solutions are able to neutralize the effects of acid production at the catalyst surface, resulting in sustained catalyst activity (Lowry and Reinhard, 2000a).

Lowry and Reinhard (2000a) also tested bicarbonate (HCO_3^-) as a potential catalyst poison. HCO_3^- is suspected as a potential poison based on aqueous phase experimental results by McNab and Ruiz (1998) and Kramer et al. (1995). Bicarbonate may also act as a catalyst poison due to its conversion to formate at the catalyst surface as illustrated by the following reaction (Lowry and Reinhard, 2000a):

$$HCO_3^- + H_2 \xrightarrow{Pd} HCO_2^- + H_2O$$

While formate itself is not a catalyst poison, carbon monoxide, which results from the Pd catalyzed conversion of formate, is a strong catalyst poison (Kramer et al., 1995). Column experiments were conducted with bicarbonate concentrations similar to the carbonate concentrations used in the experiments described in the previous paragraph. The deactivation rate constant was determined to be slightly less than (but within the same order of magnitude as) the rate constant calculated in the DI column experiment. This may be due to the increased pH at which the bicarbonate experiments were run (Lowry and Reinhard, 2000a). The results of this experiment suggest bicarbonate does not promote catalyst deactivation directly.

In each of the carbonate species column experiments (H_2CO_3, HCO_3^-, and CO_3^-), formate was detected at concentrations of 0.7 ± 0.1, 5.9 ± 0.5, and 0.6 ± 0.01 mg/L, respectively.

However, it was determined that these levels of formate were too small to produce sufficient amounts of carbon monoxide that would result in a noticeable decrease in catalyst activity (Lowry and Reinhard, 2000a).

Catalyst deactivation by hydrogen sulfide (HS^-), sulfite (SO_3^{2-}), and sulfate (SO_4^-) ions was also investigated (Lowry and Reinhard, 2000a). The presence of 0.4 mg/L HS^- decreased TCE removal efficiency from 34% to 1.8% after 5 days, while the presence of 87 mg/L SO_3^{2-} lowered TCE removal efficiency to 8.5% after 26 hours. To ensure catalyst deactivation was due to SO_3^{2-} itself, and not the reduction of SO_3^{2-} to HS^-, the column effluent was monitored for HS^-. The negative finding of HS^- in the column effluent suggests two possibilities; either SO_3^{2-} is not reduced or HS^- produced from SO_3^{2-} eludes detection due to a stronger affinity to the catalyst surface. Sulfate was tested due to speculation that it may potentially reduce to other possibly strong catalyst poisons like HS^- and SO_3^{2-}. The negative finding of reduced species in the column effluent and insignificant catalyst deactivation suggests two conclusions: sulfate neither inhibits catalyst activity nor reduces to known catalyst poisons.

Chloride (Cl^-) is yet another suspected contributor to catalyst deactivation. While chloride is a common groundwater constituent, the majority of chloride is created at the catalyst surface as a byproduct of dechlorination reactions (Lowry and Reinhard, 2000a). While Chang et al. (1999) demonstrated chloride in gas-phase dechlorination of TCE acts as a catalyst poison due to strong adsorption to the catalyst surface, column experiments performed by Lowry and Reinhard (2000) resulted in unchanged reaction rate constants

at chloride concentrations of 1003 mg/L. This however, conflicts with experimental results from Wright State University that agree with Chang et al. (1999) suggesting chloride has a strong affinity for the catalyst surface, thereby blocking available sites and reducing catalyst activity (Boggs, 2000). Column experiments performed in DI water resulted in lower than expected chloride concentrations (Boggs, 2000). It is speculated the unaccounted for chloride is strongly adsorbed to the catalyst surface, thus suppressing its detection and also effectively blocking active catalyst sites (Boggs, 2000). It is interesting to note that experiments involving larger concentrations of chloride injected into a water sample result in increased catalyst activity (Boggs, 2000; Lowry and Reinhard, 2000a). Reasons for this are unclear at this time. Table 2.5 summarizes the known effects of potential groundwater constituents on catalyst activity.

Groundwater Constituent	Effect on catalyst activity (product(s) from rxn w/ H_2)	Source(s)
oxygen (O_2)	catalyst inhibitor (water)	Kovenklioglu et al., 1992 Schreier and Reinhard, 1995 McNab et al., 2000 Lowry and Reinhard, 2000
nitrite (NO_2^-)	catalyst inhibitor (stronger than nitrate) (nitrogen, water, hydroxide ions)	Schreier and Reinhard, 1995 Lowry and Reinhard, 2000
nitrate (NO_3^-)	catalyst inhibitor (nitrogen, water, hydroxide ions)	Schreier and Reinhard, 1995 Munakata et al., 1998 Lowry and Reinhard, 2000[1]
dissolved carbon dioxide (H_2CO_3)	No adverse effect on catalyst deactivation, relative to established baseline in DI water	Munakata et al., 1998 Lowry and Reinhard, 2000
carbonate (CO_3^{2-})	No adverse effect on catalyst deactivation, relative to established baseline in DI water	Schreier and Reinhard, 1995 Munakata et al., 1998[2] Lowry and Reinhard, 2000
bicarbonate (HCO_3^-)	No adverse effect on catalyst deactivation, relative to established baseline in DI water	Lowry and Reinhard, 2000
sulfate (SO_4^{2-})	No adverse effect on catalyst activity	Lowry and Reinhard, 2000
sulfite (SO_3^{2-})	Catalyst poison	Lowry and Reinhard, 2000
hydrogen sulfide (HS^-)	Catalyst poison	Lowry and Reinhard, 2000
sulfide (S^{2-})	Catalyst poison	Boggs, 2000
chloride (Cl^-)	Strongly adsorbs to catalyst surface decreasing activity; higher concentrations result in inc. activity	Schreier and Reinhard, 1995 Boggs, 2000 Lowry and Reinhard, 2000[3]
phosphate (PO_4^{3-})	Minor catalyst deactivation observed	Munakata et al., 1998
bisulfide	Catalyst poison	Schreier and Reinhard, 1995
carbon monoxide (CO)	Catalyst poison formed from the disassociation of formate at the catalyst surface	Kramer et al., 1995

[1] - Lowry and Reinhard (2000b) reported no effect on TCE destruction at high nitrate conc. (80 mg/L)

[2] - Munakata et al. (1998) reported significant catalyst deactivation in the presence of sodium carbonate

[3] - Lowry and Reinhard (2000a) report no effect on TCE destruction at high Cl^- conc. (1003 mg/L)

Table 2.5 Common groundwater constituents and their effect on catalyst activity

2.3.5 CATALYST REGENERATION

Due to observations of catalyst deactivation (Reinhard, and Schreier, 1995; McNab and Ruiz, 1998; Lowry and Reinhard, 1999; Munakata et al. 1998; Lowry and Reinhard, 2000a), research has been dedicated to developing catalyst regeneration methods necessary for successful long-term field application. In addition to prolonging the catalyst's life, successful catalyst regeneration can also increase operator control in optimizing the system's performance.

Munakata et al. (1998) increased catalyst activity from 5% to 20% by flushing the catalyst (Pd/Al) containing column with deionized water. Nearly complete recovery of catalyst activity was achieved by placing the deactivated catalyst in a 0.07 mm Hg vacuum for 2.0 minutes prior to an oxygen flow for 15 minutes. Both phases were conducted at 300°C. Despite nearly complete catalyst recovery, 25% of the catalyst's mass was lost. The energy intensiveness of these operations, coupled with the observed catalyst loss, make it somewhat impractical for catalyst recovery in the field.

McNab and Ruiz (1998) performed successful catalyst regeneration by allowing the catalyst to soak in deionized water for a period of hours to days. Taking the electrolytically produced hydrogen off-line during regeneration to prevent contact between the catalyst and hydrogen may also have improved regeneration efforts (McNab and Ruiz, 1998). McNab and Ruiz (2000) later incorporated this latter regeneration method in addition to resting the system for a number of days between daily operations in

an attempt to prolong catalyst activity in a pilot-scale project at LLNL. Results at LLNL are discussed in greater detail in Section 2.5.

Lowry and Reinhard (2000a) conducted regeneration experiments by flushing the catalyst filled column with 90-minute pulses of dilute sodium hypochlorite (approximately 21 pore volumes). Depending on the sodium hypochlorite concentration, this oxidative treatment restored diminished catalyst activity to levels observed near the beginning of the experiments. Complete catalyst regeneration was accomplished with pulses of 750 mg/L of sodium hypochlorite solution.

Regenerations performed with lower sodium hypochlorite concentrations (75 mg/L) following experiments with DI water and TCE and DI water, TCE, and other known catalyst poisons like HS^- and SO_3^{2-} (Lowry and Reinhard, 2000a) resulted in partial regeneration. This suggests the extent to which catalyst activity is restored may be dependent on the hypochlorite concentration (Lowry and Reinhard, 2000a).

2.4 MODELING Pd/H_2 HYDRODEHALOGENATION

In addition to enhancing understanding by describing the major processes influencing system behavior, models can also be used as management tools for optimizing cost and performance. This section describes modeling that has been conducted to describe the destruction of chlorinated ethenes via the Pd/H_2 system. In this section, we also discuss different methods that may be applied to simulate catalyst deactivation due to poisoning. As noted in Section 2.3.2.1, so long as H_2 concentrations are greater than approximately

1 mM, competition for H_2 by other species (O_2, nitrate, and nitrite) does not lead to reduction of TCE conversion. Since sparging with H_2 gas results in dissolved H_2 of 1mM (Lowry and Reinhard, 2000a), it may be assumed that for technology implementation, competition for H_2 will not reduce the efficiency of the Pd/H_2 system. Therefore, catalyst inhibition due to competition for H_2 will not be modeled. This assumption is discussed further in Chapter 3.

Pseudo-first-order kinetics have been used to describe the destruction of chlorinated ethenes (C_a) in the Pd/H_2 system (Schreier and Reinhard, 1995; Lowry and Reinhard, 1999; Lowry, 2000). That is, the rate at which chlorinated ethenes are destroyed (dC_a/dt) can be described by the following expression, where k_{obs} is a first-order rate constant with units of (T^{-1}).

$$\frac{dC_a}{dt} = -k_{obs}C_a \qquad (1)$$

The observed rate constant, k_{obs}, is determined by integrating equation (1) as contaminated water flows through a column and solving for k_{obs} (Lowry and Reinhard, 2000a):

$$k_{obs} = -\frac{\ln \frac{C_{eff}}{C_{in}}}{t_r} \qquad (2)$$

where t_r represents the residence time of the fluid in the column. Lowry and Reinhard (1999) modified the first-order model in equation (1) into a pseudo-first-order model to account for the concentration of Pd/Al catalyst (C_{cat}) present in batch experiments:

$$-\frac{1}{C_{cat}}\frac{dC_a}{dt} = k_{rxn}C_a \qquad (3)$$

where k_{rxn} is the observed first-order rate constant (k_{obs}) normalized by the catalyst concentration (C_{cat}). Equation (3) accounts for the fact that the contaminant removal rate was proportional to catalyst concentration in the batch system (Lowry and Reinhard, 1999). Dividing by the catalyst concentration normalizes the chlorinated ethene destruction rate to account for varying catalyst concentrations in different experiments. Note that the units of the rate constant k_{rxn} are now $[L^3M^{-1}T^{-1}]$.

If reaction conditions are such that first-order kinetics dictate the rate at which contaminant transformation occurs, the rate constant will remain the same, regardless of C_{in}. However, as C_{in} increases beyond the catalyst's ability to vacate sites for dechlorination, the reaction becomes zero-order. Lowry validated the assumption of pseudo-first-order kinetics at TCE concentrations up to 19.4 mg/L in column experiments performed with 0.5 g Pd/Al catalyst (Lowry, 2000).

Lowry also validated the assumption of pseudo-first-order kinetics with respect to catalyst mass. Column experiments performed with various amounts of Pd/Al catalyst (0.25 – 4 g) resulted in a linear relationship between catalyst mass and k_{obs}. It is important to note that the residence time used to calculate k_{obs} includes the effective porosity (void space external to the catalyst) and not the total porosity (void space internal and external to the catalyst). This was justified by assuming that fluid flow through the catalyst pores (80% of which are less than 8 nm) is not substantial and therefore does not contribute to increasing the residence time.

It is also important to note that k_{obs} is calculated under the assumption that plug flow conditions exist throughout the column. This assumption becomes invalid at low flow rates due to mass transfer resistance resulting from slower velocities through the column and increased contaminant axial dispersion. Under these conditions, it is more likely the true pseudo-first-order rate constant is underestimated (Lowry, 2000; Boggs, 2000). Lowry (2000) calculated a rate constant of approximately 1.0 min^{-1} for a column (10.5 ml) fully packed with 7.3 g Pd/Al. While this value contains the effects of axial dispersion and mass transfer resistance, it provides us with a conservative estimate of contaminant destruction, which will be incorporated into a model describing palladium-catalyzed destruction of chlorinated ethenes, presented in Chapter 3.

While the pseudo-first-order model generally fits the data, it under predicts TCE conversion to ethane in the early stages of an experiment and over predicts the conversion in later stages (Lowry and Reinhard, 1999). This inconsistency of model predictions and experimental results may be due to catalyst deactivation, which is not accounted for in the pseudo-first-order model.

To account for catalyst deactivation, Lowry and Reinhard (2000a) developed a model describing catalyst deactivation using the methods of Levenspiel for flow through a catalyst-filled column (Lowry and Reinhard, 2000a; Levenspiel, 1999)

$$\frac{g_{cat}}{Q} = \frac{1}{k_{rxn} e^{-k_d t}} \ln \frac{C_{in}}{C_{eff}} \qquad (4)$$

where g_{cat} is the mass of catalyst in the column ($M_{catalyst}$), Q is the fluid flow rate (L^3/T), C_{in} is the concentration of target contaminant entering the column ($M_{contaminant}/L^3$), and

C_{eff} is the effluent target contaminant concentration ($M_{contaminant}/L^3$). Recall, we defined k_{rxn} as the first-order rate constant, normalized by catalyst concentration. For their column experiments, Lowry and Reinhard (2000a) defined k_{rxn} as follows:

$$k_{rxn} = \frac{k_{obs}}{\frac{g_{cat}}{nV}} \tag{5}$$

where n represents the porosity of the catalyst column and V is the empty column volume. Equation (4) assumes the first-order rate constant (k_{rxn}) decreases exponentially (at the deactivation rate constant, k_d), where k_{rxn} is determined from equations (2) and (5). The catalyst deactivation rate constant, k_d (T^{-1}) is determined by first linearizing equation (4) to obtain the following form:

$$\ln\ln\left(\frac{C_{in}}{C_{eff}}\right) = \ln\left(\frac{k_{rxn}g_{cat}}{Q}\right) - k_d t \tag{6}$$

In this form, k_d is the slope of the best-fit line through data obtained from column experiments.

As stated earlier, Lowry and Reinhard (2000a) used k_d to quantify the degree of catalyst deactivation in various water matrices. Table 2.6 lists the deactivation rate constants (k_d) determined by Lowry and Reinhard (2000a) for various groundwater constituents. These calculations were made based on column experiments performed with a TCE influent concentration of approximately 3.5 mg/L and a flow rate of 1 ml/min. Those compounds with deactivation rate constants greater than the baseline (5.6×10^{-3} day^{-1}) by two orders of magnitude were identified as likely catalyst poisons (Lowry and Reinhard, 2000a).

Solute	[Solute] (mg/L)	k_d ($day^{-1} \times 10^3$)
none (DI)	--	5.6
H_2CO_3	580	2.8
HCO_3^-	660	5
CO_3^{2-}	659	2.1
SO_4^-	690	7.6
SO_3^{2-}	87	>500[b]
	44[a]	>900[b]
HS^-	0.4	424
	0.8[a]	>2000[b]
Cl^-	1003	3.7

[a] - Two concentrations were used for SO_3^{2-} and HS^-

[b] - too few data points available to get accurate measure of k_d

Table 2.6 Deactivation rate constants for various groundwater constituents (Lowry and Reinhard, 2000b)

While Levenspiel's model (equations (4) and (5)) accurately fits the data from Lowry and Reinhard's (2000a) column experiments, the model does not account for the effect of aqueous hydrogen concentration on contaminant destruction. Lowry and Reinhard (2000b) later developed a Langmuir-Hinshelwood kinetic model to describe the relationship between aqueous hydrogen and TCE destruction.

$$-\frac{dC_{TCE}}{dt}\cdot\frac{1}{c_{cat}} = k_{rxn}\left(\frac{K_{TCE}C_{TCE}}{1+K_{TCE}C_{TCE}}\right)\left(\frac{K_{H_2}^n C_{H_2}^n}{1+K_{H_2}^n C_{H_2}^n}\right) \qquad (7)$$

In equation (7), k_{rxn} is the apparent reaction rate constant with units of ($M_{contaminant}M_{catalyst}^{-1}T^{-1}$); where c_{cat} is the catalyst concentration; C_{TCE} and C_{H2} are the TCE and hydrogen concentration, respectively; and n is an exponent set equal to 1 for molecular adsorption of hydrogen and 0.5 for disassociative adsorption of hydrogen, based on previous modeling of the hydrogenation of aqueous nitrate using a Pd/Cu catalyst (Pintar et al. 1996). K_{TCE} and K_{H2} are equilibrium adsorption constants for TCE and hydrogen, respectively, having units of (L^3/M).

Due to the fast reaction rates exhibited by the Pd/H_2 system, K_{TCE} is extremely low (i.e. $K_{TCE}C_{TCE} << 1$) which allows us to make the following simplification and rearrangement:

$$\frac{dC_{TCE}}{dt} \cdot \frac{1}{c_{cat}} = -k_{obs} C_{TCE} \tag{8}$$

where

$$k_{obs} = -k_{rxn} K_{TCE} \left(\frac{K_{H_2}^n C_{H_2}^n}{1 + K_{H_2}^n C_{H_2}^n} \right) \tag{9}$$

While this model incorporates the effect of aqueous hydrogen on the observed rate constant, it does not take into consideration catalyst deactivation. Also note that if H_2 is assumed not to be limiting, $K_{H_2}^n C_{H_2}^n >> 1$, and k_{obs} is independent of H_2 concentration. Chang et al. (1999) used various kinetic expressions to model the hydrodechlorination of 1,2-dichloroethane (1,2-DCA) on a Rh/SiO_2 catalyst, but were unsuccessful in attaining a good fit to experimental results. This was due to the models' inability to account for catalyst deactivation. During hydrodechlorination, the chloride ions (Cl^-) originally in the 1,2-DCA molecule separate and adsorb to the catalyst surface. This adsorption decreases the number of available sites for dechlorination, thereby deactivating the catalyst. Once bound to the catalyst surface, Chang et al. (1999) speculated that these chloride ions would react with hydrogen ions created from the disassociation of hydrogen gas (H_2) at the catalyst surface to produce gaseous HCl.

Chang et al. (1999) presented a modified first-order model to describe the dechlorination of 1,2-DCA on a Rh/SiO_2 catalyst. The model incorporated two assumptions. First, 1,2-DCA conversion was assumed to be proportional to the fraction of available catalyst sites (θ_v). Second, θ_v was assumed to be is inversely proportional to the gaseous partial pressure of the catalyst poison, HCl. Therefore, if the gaseous partial pressure of HCl is

low, θ_v is high, resulting in contaminant conversion at or near maximum potential. Conversely, if the gaseous partial pressure of HCl is high, contaminant conversion is reduced due to a decrease in θ_v. These two assumptions will be applied in Chapter 3 to develop a model of palladium-catalyzed destruction of chlorinated ethenes.

2.5 FIELD APPLICATIONS

Successful application of the Pd/H_2 system has been demonstrated at LLNL for over a year (McNab et al., 2000). The decision to incorporate a Pd/H_2 system resulted from site-specific conditions negating the use of current remediation technologies. The presence of tritium in the contaminated groundwater eliminated pump and treat as a viable alternative due to the unacceptability of pumping tritiated water to the surface. Due to aerobic conditions in the contaminated portion of the aquifer and large depths to the contaminant plume (>40 m) monitored natural attenuation and permeable reactive barriers were eliminated as potential remediation strategies (McNab et al., 2000). Figure 2.2 is a schematic showing the in-well Pd/H_2 system (McNab et al., 2000).

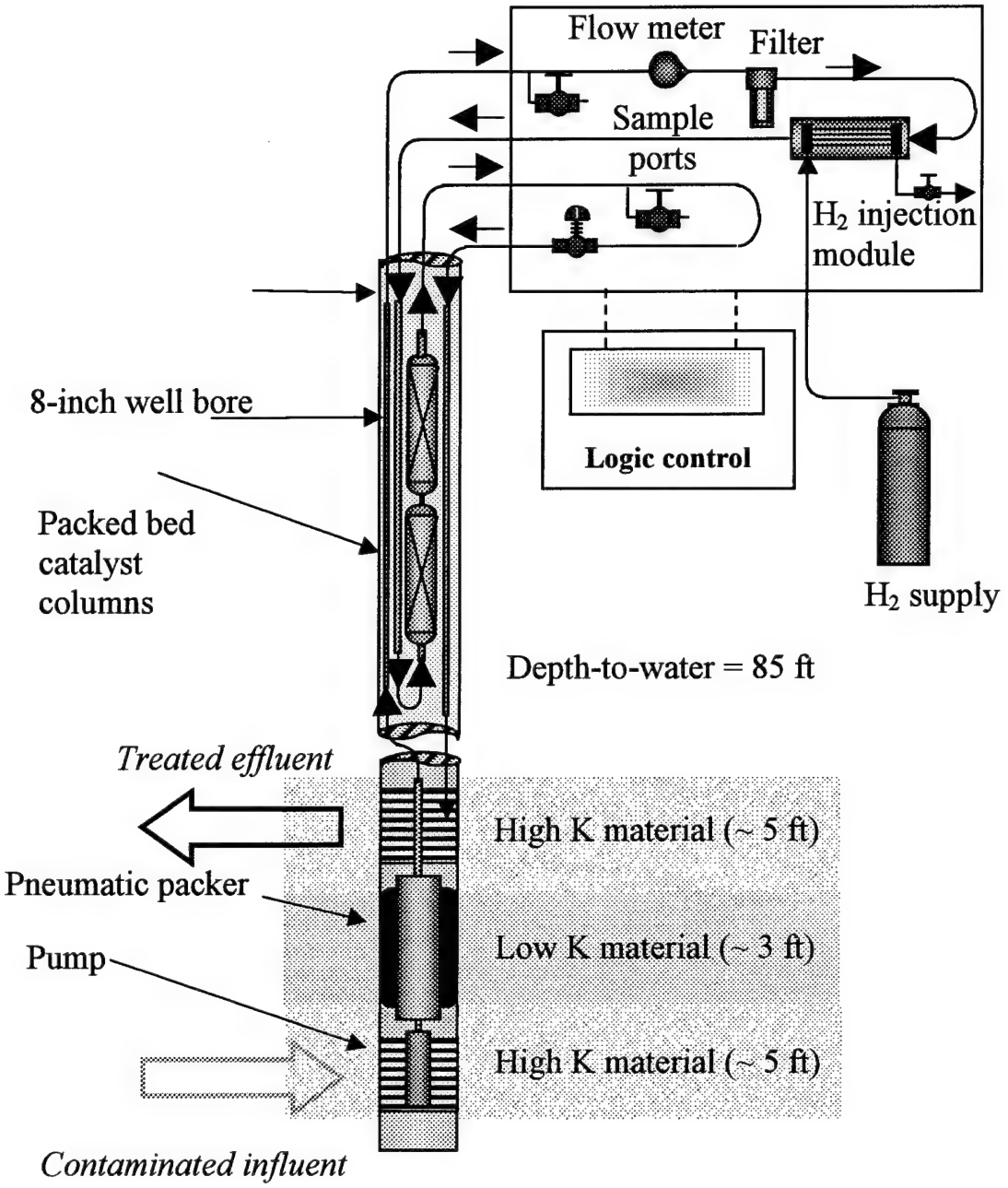

Figure 2.2 Schematic of Pd/H_2 system using in-well catalytic reactors (McNab et al., 2000)

The groundwater is saturated with hydrogen gas prior to flowing through two stainless steel columns filled with Pd/Al. The first column was designed to perform most of the contaminant destruction, while the second column was added as a polishing reactor. Sample ports were installed in the influent stream, after the H_2 injection module, and in

the effluent streams of each catalytic column to monitor system efficiency. Prior subsurface investigations indicated an area within the contaminated plume of two distinct sand layers, separated by an impermeable clay layer. Each sand layer contained similar concentration levels of contaminants (PCE, TCE, 1,1-DCE were among the chlorinated ethenes detected) (McNab et al., 2000). Contaminated groundwater was drawn from the lower sand layer and discharged through the upper sand layer, where infiltration back to the lower layer was prevented due to the presence of the clay layer (McNab et al., 2000). A pneumatic packer was installed to prevent flow short-circuiting. The Pd/H_2 system ran for 4 hr/day during initial operations. The first column alone reduced PCE; TCE; and 1,1-DCE by more than 99%. Other CHC's like chloroform and carbon tetrachloride were effectively destroyed also (91% and >98%, respectively) (McNab et al., 2000). Consistent with prior studies by Lowry and Reinhard (1999), 1,2-DCA displayed strong resistance to dechlorination (McNab et al., 2000). The lack of noticeable cis-DCE destruction is most likely due to incomplete TCE and PCE destruction at the catalyst surface. Regeneration was performed at the end of daily operation by flushing the catalyst column with three pore volumes of non-hydrogenated water and then draining the column to allow exposure to the air above the water table. It is speculated that exposure to air does not regenerate catalyst activity, but rather prevents further deactivation due to adsorption of unwanted groundwater constituents to the catalyst surface. In addition to daily regeneration, the column was flushed with DI water at the end of every week.

Daily system operation was increased to 8 hr/day for 5 days/week after the first 20 days of initial testing. Contaminant breakthrough along with the production of VC was observed within 10 days of operating at this new schedule (McNab et al., 2000). In order to restore system efficiency, daily operation was reduced to 4 hr/day. In addition, the standard 5-day operation schedule was reduced to shorter operation periods of 1 – 3 days, while the rest period was increased from 2 to 5 days. It was later shown that the system could operate as much as 5 - 6 hours daily for 5 days a week with similar contaminant destruction efficiencies (McNab et al., 2000).

Sampling the first column's effluent indicated nearly complete hydrogen utilization due to either catalytic hydrodehalogenation or hydrogen combining with O_2 at the catalyst surface to form water. The absence of hydrogen entering the second catalyst column resulted in no contaminant destruction in that column. Water flow through the two columns was adjusted by alternating the water flow (bottom-up to top-down) every 4 – 5 hours so as to equally utilize both catalytic columns. This dramatically improved the system by allowing the system to operate for nearly double the hours before both columns were deactivated (McNab et al., 2000). This field demonstration proves the Pd/H_2 system's ability to sustain effective contaminant removal efficiencies for an extended period of time (McNab et al., 2000).

2.6 HORIZONTAL FLOW TREATMENT WELLS (HFTWs)

As mentioned in Chapter 1, HFTWs can be incorporated into a remediation strategy based on these systems' abilities to control plume migration and increase treatment

efficiency by causing multiple passes of contaminant through an established treatment technology. Chapter 1 also briefly mentioned the successful use of HFTWs at Edwards AFB, CA. This particular system moved groundwater multiple times through a bioremediation zone (McCarty et al., 1998). In the Pd/H_2 system, the contaminant is passed through catalyst columns residing in the well bores of the HFTW system. Although the residence time in the columns is minimal, treatment is effective due to the fast reaction kinetics of the Pd/H_2 system. In this section, we will describe the HFTW system in greater detail. We will also look at the HFTW model presented by Christ (1997) as well as Ferland's (2000) model that incorporates catalytic destruction of TCE using Pd/H_2 reactors in an HFTW system.

For an HFTW system to properly work, vertical movement of groundwater between the injection and extraction screens of a single treatment well should be minimal. This is typically found to be the case, since most aquifers exhibit horizontal hydraulic conductivities an order of magnitude greater than vertical hydraulic conductivities (Domenico and Schwartz, 1998). The assumption that flow is horizontal is important as it allows us to model the system as two separate injection/extraction well pairs working simultaneously. Figure 2.3 illustrates a two-well HFTW system showing one injection/extraction well pair in the lower aquifer, where downflow and upflow treatment wells are injecting and extracting water, respectively. Similarly, in the upper aquifer, the upflow well serves to inject water and the downflow well extracts water.

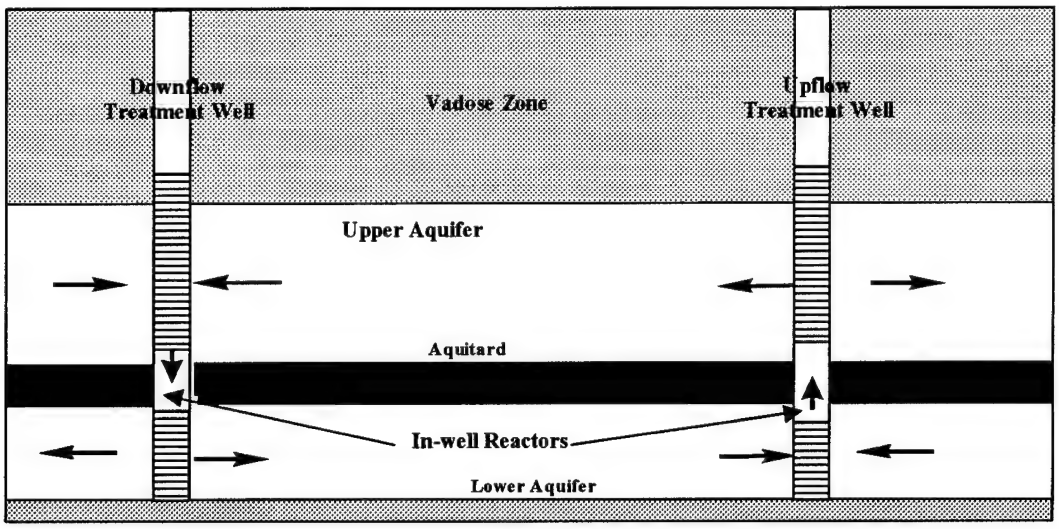

Figure 2.3 HFTW operating in two aquifers (after Ferland, 2000)

Now that the concept of an HFTW system has been described, let us define five important variables that will be used in determining system performance: interflow (I_U, I_L, and I_T), capture zone width (CZW), treatment efficiencies (η_{spU}, η_{spL}, and $\eta_{overall}$), upgradient concentration (C_{in}), and downgradient concentrations (C_{outL}, C_{outU}). Figure 2.4 is a plan view of the upper aquifer portion of Figure 2.3.

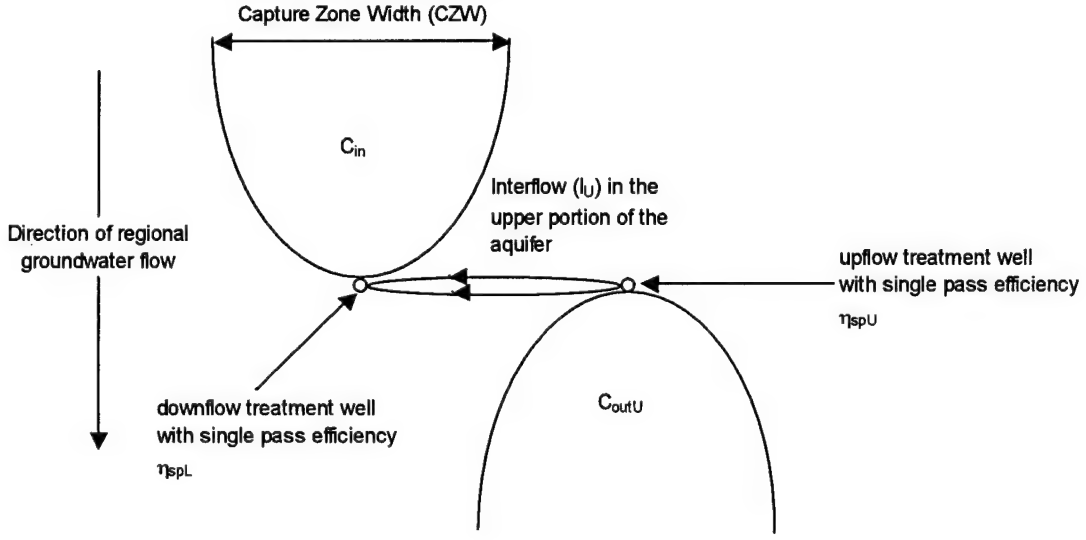

Figure 2.4 Plan view of 2-well HFTW system (upper aquifer shown)

Interflow is defined as the fraction of the total groundwater pumped through an extraction screen that originated from the injection screen of an adjacent treatment well. I_U and I_L define the interflow between upper and lower screens in the aquifer, respectively. As seen in Figure 2.4, interflow travels toward the downflow treatment well in the upper aquifer. Interflow always travels from an injection screen to an extraction screen. Therefore, in a two-well pair HFTW, interflow in the upper and lower portions of the aquifer will be in opposite directions.

The outer envelope of groundwater streamlines that converge on a well is the capture zone curve. The capture zone width (CZW) is the width perpendicular to the direction of regional groundwater flow of the capture zone curve of a treatment well. If the CZW is less than the estimated contaminated plume width, additional well pairs may be installed to increase the overall CZW. Christ (1997) calculated the CZW as:

$$CZW = \frac{Q}{UB}\left[\frac{N}{2} - I_T\right] \tag{10}$$

where

Q	=	pumping rate of a single treatment well
U	=	groundwater Darcy velocity through aquifer
B	=	depth of aquifer
N	=	number of wells
I_T	=	ratio of flow through all extraction wells originating from injection wells and the total flow through a single extraction well

Interflow (I_U, I_L, and I_T) for a given aquifer and HFTW configuration is determined using complex potential theory. This calculation is beyond the scope of the current study. The interested reader is referred to Christ (1997) and Christ et al. (1999) for further information.

Single pass treatment efficiency (η_{sp}) is defined as the fraction of contaminant destroyed following a single pass through the Pd/H_2 treatment column. For the two-well HFTW system, two treatment efficiencies are used: η_{spU} and η_{spL}. The parameter η_{spU} represents the contaminant destruction efficiency of the catalyst column residing in the upflow treatment well, while η_{spL} represents the destruction efficiency of the catalyst column residing in the downflow treatment well.

C_{in} refers to the upgradient contaminant concentration entering the HFTW system. Note that it is assumed C_{in} entering the HFTW system is equal in the upper and lower sections of the aquifer. The contaminant concentrations exiting the HFTW system consist of the concentration in the upper and lower section of the aquifer, C_{outU} and C_{outL}, respectively. Christ (1997) used mass-balance to determine C_{outU} and C_{outL} based on C_{in}, I_U, I_L, η_{spU}, and η_{spL} as seen in equations (11) and (12).

$$C_{outU} = C_{in}\left[\frac{(1-I_L)(1-\eta_{spU})+I_L(1-I_U)(1-\eta_{spL})(1-\eta_{spU})}{1-I_U I_L(1-\eta_{spL})(1-\eta_{spU})}\right] \tag{11}$$

$$C_{outL} = C_{in}\left[\frac{(1-I_U)(1-\eta_{spL})+I_U(1-I_L)(1-\eta_{spL})(1-\eta_{spU})}{1-I_U I_L(1-\eta_{spL})(1-\eta_{spU})}\right] \tag{12}$$

where η_{spU} = single pass treatment efficiency through treatment reactor in upflow well
η_{spL} = single pass treatment efficiency through treatment reactor in downflow well
I_U = average interflow between upper screened wells
I_L = average interflow between lower screened wells
C_{in} = influent (upgradient) contaminant concentration
C_{outL} = contaminant concentration exiting treatment system in lower aquifer
C_{outU} = contaminant concentration exiting treatment system in upper aquifer

If $C_{outL} = C_{outU} = C_{down}$, we can define the overall contaminant removal efficiency as:

$$\eta_{overall} = 1 - \frac{C_{down}}{C_{in}} \tag{13}$$

2.6.1 FERLAND'S (2000) Pd/H_2 REACTOR SUBMODEL

Ferland (2000) incorporated a first-order rate model to describe contaminant destruction within an in-well palladium reactor. The single pass treatment efficiency (η_{sp}) for the reactor with volume (V), reactor porosity (n), pumping rate (Q) and a first-order rate constant (k) is seen in equation (14):

$$\eta_{sp} = 1 - e^{\left(-k\frac{Vn}{Q}\right)} \tag{14}$$

Note that Vn/Q is simply the hydraulic residence time (t_r) within the reactor. This approach is used for determining both single pass efficiencies in the HFTW system: η_{spU} and η_{spL}. The overall system efficiency in the upper and lower aquifer may then be calculated using equations (11) and (12) based on η_{spU}, η_{spL}, and the interflows (I_U and I_L) between the well pair. A more in-depth discussion of this calculation will be presented in Chapter 3. Figure 2.5 (after Ferland, 2000) is a non-dimensional contour plot illustrating

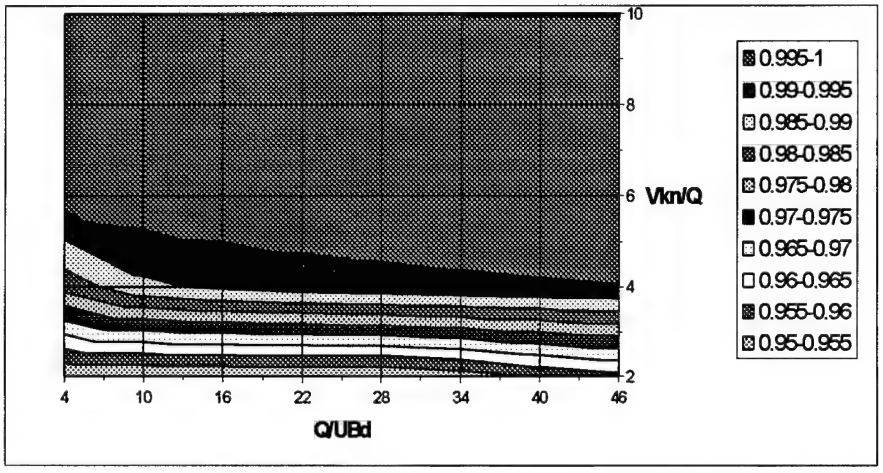

Figure 2.5 HFTW efficiency contour plot at α = 67.5 deg (after Ferland, 2000)

HFTW efficiencies based on the pumping rate (Q), regional aquifer groundwater velocity (U), aquifer thickness (B), half distance separating treatment wells (d), empty reactor volume (V), first-order reaction rate constant (k), and column porosity (n). Note that Figure 2.6 is constructed based on a specific well pair orientation with respect to the regional groundwater flow direction (α).

Ferland's (2000) model used a first-order rate constant based on previously published field data (McNab et al., 2000) to simulate contaminant destruction in the in-well reactors of the HFTW system. While this rate constant accurately reflects operational results, it does not account for catalyst deactivation, which essentially lowers the rate constant over time. This thesis effort will extend Ferland's (2000) simple first-order reaction submodel by incorporating a Pd/H_2 reactor submodel that simulates catalyst deactivation as a function of contaminant concentration, groundwater composition, and pumping rate. Catalyst regeneration will also be simulated.

3.0 METHODOLOGY

3.1 INTRODUCTION

In this chapter, a model is presented to simulate the in situ destruction of chlorinated ethene contaminants using in-well Pd/H_2 reactors in an HFTW system. The chapter begins with development of a submodel to simulate the single pass treatment efficiency of an in-well Pd/H_2 reactor. The reactor submodel is then incorporated into Ferland's (2000) HFTW flow model. In the remainder of the chapter, a methodology is laid out describing how the model will be applied to help us gain a better understanding of how in-well Pd/H_2 reactors can be used to remediate chlorinated ethene contaminated groundwater.

3.2 IN-WELL Pd/H_2 REACTOR SUBMODEL

3.2.1 MODEL ASSUMPTIONS

(1) Contaminated groundwater is saturated with aqueous hydrogen gas prior to flowing through the Pd/H_2 reactor. This assumption simplifies the submodel in two ways. First, an abundant supply of hydrogen, such that $K_{H_2}^n C_{H_2}^n >> 1$, reduces the second order reaction equations (7) and (8) to a first-order model. Second, the effects of other solutes that compete for hydrogen (e.g. oxygen and nitrite) are minimized and assumed insignificant (Lowry and Reinhard, 2000b).

(2) Catalyst regeneration is instantaneous. The time scale of catalyst deactivation (weeks to months), relative to the regeneration time scale (minutes) (Lowry and Reinhard, 2000a) allows us to make this simplification.

(3) Catalyst regeneration results in complete recovery of catalyst sites lost to catalyst deactivation. As a result, contaminant removal efficiencies after regeneration will equal efficiencies attained at the beginning of the simulation. Complete recovery of catalyst sites lost to catalyst poisoning has been observed by pulsing the Pd reactor with relatively high concentrations (750 mg/L) of sodium hypochlorite (Lowry and Reinhard, 2000a). However, additional research is needed to accurately determine the relationship between the regenerating agent concentration and recovery of deactivated catalyst sites.

(4) Although chlorinated ethene destruction is based from experimental column results of TCE destruction in DI water (Lowry and Reinhard, 2000a), destruction efficiency for other (PCE, DCE, and VC) is assumed to be similar.

(5) The decrease in k_{obs} is negligible during the time contaminated water spends in the catalyst reactor. In other words, the catalyst deactivation time scale is much larger than the reactor residence time.

(6) The 2 – 3 day period of catalyst super activity observed at the beginning of column experiments (and after subsequent regenerations) will not be modeled (Lowry and Reinhard, 2000a). This phenomenon was repeatedly observed in column studies performed by Lowry and Reinhard (2000a) and is common in most heterogeneous catalytic systems. Reasons for this behavior may be due to microscale changes on

the catalyst surface. However, the phenomenon is transient and not deemed significant for long-term analysis.

(7) The effect of groundwater pH on contaminant destruction efficiency in the Pd column is deemed negligible and is not considered in the submodel. The minimal change observed in contaminant destruction efficiency for a 7 unit range of pH (Lowry and Reinhard, 2000a) validates this assumption.

(8) The catalyst deactivation rate constant (k_d) is proportional to the mass loading of influent contaminant/catalyst poison ($Q_{in}C_{in}$) and inversely proportional to the amount of catalyst (g_{cat}) used in the reactor.

(9) A poison's ability to deactivate the catalyst is constant whether it acts alone or in conjunction with additional poisons. In other words, competition for catalyst sites among multiple poisons will not change an individual poison's affinity to the catalyst surface. This assumption allows us to calculate a single k_d as the sum of the k_ds of individual poisons to quantify the effect of catalyst deactivation resulting from multiple groundwater constituents.

(10) Mass transfer resistances are considered negligible in this submodel. Mass transfer resistance was detected at relatively low flow velocities (0.3 – 4.0 cm/min) (Lowry, 2000). However, resistance is expected to diminish as flow velocity increases. At the relatively high flow velocities that would be encountered in an in-

well reactor (20 – 35 cm/min) it is anticipated that mass transfer resistance would be negligible.

3.2.2 MODELING CATALYST DEACTIVATION

As stated in Chapter 2, contaminant destruction in the Pd/H_2 system has been modeled using first-order kinetics (equation 1). Solving equation (1) yields the following equation for contaminant concentration exiting the catalyst column:

$$C_{eff} = C_{in} e^{-k_{obs} t_r} \qquad (15)$$

where C_{in} represents influent contaminant concentration, C_{eff} is the effluent contaminant concentration, k_{obs} is the first-order reaction rate constant, and t_r is the residence time in the catalyst reactor. However, first-order models that use a single rate constant are based on the assumption that catalyst activity remains constant. As shown in the previous chapter, catalyst deactivation is an important process that should be simulated. In this modeling study, catalyst deactivation is incorporated into a first-order model by considering the first-order rate constant (k_{obs}) as a function of time. At any moment in time, a first-order rate constant quantifies contaminant destruction in the Pd/H_2 reactor, which allows us to calculate the effluent concentration using equation (15). As time progresses, the rate constant decreases leading to a decrease in catalyst efficiency.

We now need to decide how to model the decrease in the first-order rate constant, k_{obs}, over time. Following Chang et al. (1999), we assume the rate constant is proportional to the fraction of catalyst sites available for contaminant destruction (θ_v), such that

$$k_{obs}(t) = k_{obs0} \cdot \theta_v(t) \tag{16}$$

where k_{obs0} is the first-order rate constant (min^{-1}) observed after the initial 2 – 3 day period of catalyst super activity (Lowry and Reinhard, 2000a) and t is time measured in days. Table 3.1 illustrates first-order reaction rate constant values (Lowry and Reinhard, 2000a) for column experiments analyzing TCE destruction efficiency in the presence of various catalyst poisons.

Contaminant/ Solute	concentrate (mg/L)	k_{rxn} ($ml\ g_{cat}^{-1} min^{-1}$)
TCE	3.5	0.77 - 0.56
SO_3^{2-}	44	0.76 - 0.02
HS^-	0.4	0.85 - 0.04

Table 3.1 First-order reaction rate constants for various contaminant/solute concentrations (Lowry and Reinhard, 2000a)

In order to model $\theta_v(t)$ with time, we first rewrite equation (4):

$$\eta_{sp}(t) = 1 - e^{-\left[\frac{g_{cat} \cdot k_{rxn}}{Q \cdot e^{k_d t}}\right]} \tag{17}$$

Equation (17) is how Lowry and Reinhard (2000a) modeled the decrease in catalyst destruction efficiency due to catalyst deactivation. If we now assume that this decrease in destruction efficiency is due to a decrease in available catalyst sites, we can calculate $\theta_v(t)$ as follows:

$$\theta_v(t) = \frac{1 - e^{-\left[\frac{g_{cat} \cdot k_{rxn}}{Q \cdot e^{k_d t}}\right]}}{1 - e^{-\left[\frac{g_{cat} \cdot k_{rxn}}{Q}\right]}} \tag{18}$$

Substituting equation (5) for k_{rxn} in equation (18) and canceling like terms gives us

$$\theta_v(t) = \frac{1 - e^{-\left[\frac{k_{obs0} \cdot t_r}{e^{k_d t}}\right]}}{1 - e^{-[k_{obs0} \cdot t_r]}} \tag{19}$$

Close examination of equation (18) indicates that $\theta_v = 1$ at $t = 0$, indicating all catalyst sites are available for contaminant destruction, as expected initially. The rate at which catalyst sites become deactivated is dependent upon the deactivation rate constant, k_d. Deactivation rate constants determined by Lowry and Reinhard (2000a) are used as a baseline for calculating k_d values that are specific to reaction conditions (catalyst mass and contaminant/poison loading) in the catalyst reactor. As noted in assumption 7, k_d is assumed proportional to the contaminant/poison mass loading and inversely proportional to catalyst mass. Based on Lowry and Reinhard's (2000a) column studies, Table 3.1 lists the k_d values used in this submodel, along with the associated contaminant/poison loadings and catalyst masses that are necessary to calculate k_d values for other contaminant loadings and catalyst masses.

Catalyst Poison	[Poison Loading] (mg/min)	g_{cat} (gm)	k_d ($day^{-1} \times 10^3$)
TCE	3.5×10^{-3}	0.5	5.6
SO_3^{2-}	4.4×10^{-2}	0.5	900
HS^-	4.0×10^{-4}	0.5	424

Table 3.2 Baseline k_d values and corresponding experimental parameter values

The overall k_d value used in equation (19) is determined by summing the k_d values of the individual contaminants/poisons contributing to catalyst deactivation and is given in equation (20).

$$k_{d(Total)} = \frac{Q}{g_{cat}} \sum_{i=1}^{n} M_{kd_i} C_{in_i} \qquad (20)$$

where g_{cat} is the amount of Pd/Al catalyst used [M], M_{kd} represents the proportionality constant for the i^{th} contaminant/poison relating k_d to contaminant/poison loading and amount of catalyst used [$M_{catalyst}M_{poison}^{-1}$] , C_{in} represents the contaminant/poison

concentration [M_{poison}/L^3], and n represents the total number of contaminants and poisons in the system. Table 3.2 is a list of M-values for TCE, HS^-, and SO_3^{2-} based on the column experiments of Lowry and Reinhard (2000a).

Contaminant/Poison	M_{kd} (gm_{cat} /mg_{poison})
TCE	5.6×10^{-4}
HS^-	3.68×10^{-1}
SO_3^{2-}	7.1×10^{-3}

Table 3.3 M_{kd} values for TCE and known catalyst poisons

Once the reaction rate constant function, $k_{obs}(t)$, is known, calculating η_{sp} over time (days) is accomplished using equation (21):

$$\eta_{sp}(t) = 1 - e^{-\left[k_{obs}(t)\left(\frac{nV}{Q}\right)\right]} \tag{21}$$

where $k_{obs}(t)$ is calculated using equations (16) and (19). The reader will note that equation (21) is similar to equation (14), with the exception that the rate constant now decreases with time in order to simulate catalyst deactivation. Figure 3.1 is a comparison between experimental data for TCE in DI water passing through a Pd/Al column (Lowry and Reinhard, 2000a) and submodel output from equation (21) using parameters specific to the experiment. The k_d value was calculated from equation (20) with TCE as the sole contaminant (C_{in} = 3.5 mg/L) and g_{cat} = 0.5 gm. A best fit of the data was obtained using k_{obs0} = 1.25 min^{-1}. This value corresponds to a k_{rxn} value of 0.74, which falls within the range of first-order rate constant values listed in Table 3.1.

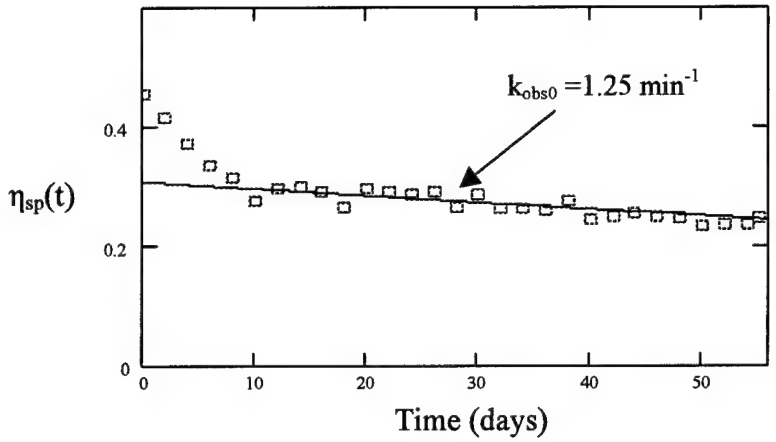

Figure 3.1 Calibrating the submodel to experimental data (Lowry and Reinhard, 2000a) TCE_{in} = 3.5 mg/L, Q = 1 ml/min, V = 0.7 ml, t_r = 0.3 min, g_{cat} = 0.5 gm

3.2.3 MODELING REGENERATION

As mentioned in Section 3.2.1, catalyst regeneration is assumed to result in complete and instantaneous recovery of catalyst sites lost to deactivation. Regeneration at time r is simulated as follows:

$$\theta_v(t) = \theta_v(t-r) \quad \text{for } t \geq r \qquad (22)$$

Assuming C_{in} and Q are the same before and after regeneration, contaminant destruction efficiency after regeneration will be the same as the efficiency observed at the beginning of system operation. Figure 3.2 is an illustration that extends the column experiment shown in Figure 3.1 to include three regenerations at days 58, 82, and 102, respectively.

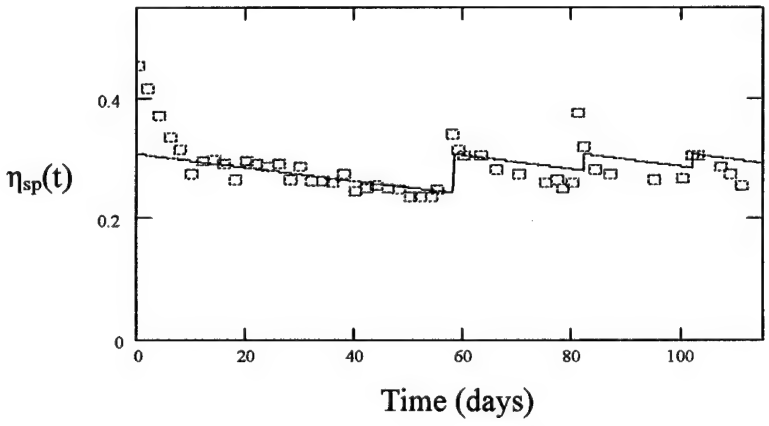

Figure 3.2 Submodel output including multiple catalyst regenerations

3.2.4 SUBMODEL LIMITATIONS

While this submodel is able to account for processes in the Pd/H_2 system like catalyst deactivation and regeneration, limitations exist. Bacteria growth on the catalyst surface is not considered, but may contribute significantly to deactivation, as was thought to be the case of groundwater tested from Moffett Field (Lowry and Reinhard, 2000a). Detection of VC in the column effluent as the result of incomplete dechlorination at the catalyst surface is possible due to insufficient aqueous hydrogen gas (Lowry and Reinhard, 2000b) or catalyst deactivation (Lowry and Reinhard, 1999; McNab and Ruiz, 2000). While the submodel calculates efficiency based on the fraction of influent contaminant destroyed, daughter product production is not considered.

As previously mentioned, this submodel is designed to predict TCE destruction in the catalyst column. The treatment system's ability to destroy other chlorinated ethenes like PCE, DCE, and VC is expected to be similar to TCE destruction rates based on experimental results by Lowry and Reinhard (1999) (Table 2.1). In order to more accurately predict contaminant destruction, further research is needed to obtain k_d values for other chlorinated ethenes and suspected catalyst poisons.

The submodel predicts contaminant destruction efficiency based on a Pd reactor packed with the specific Pd/Al beads used in the Lowry and Reinhard (2000a) column studies (1.6 mm diameter, 1% Pd). Therefore, this submodel may not be applicable to differently configured catalyst beads. Using a smaller catalyst bead would likely reduce the rate of catalyst deactivation (i.e. greater surface area and more catalyst sites) as well as reduce

mass transfer limitations (Clark, 1996). However, the pumping energy required to overcome additional headloss on groundwater pumped through the reactor makes the smaller bead an unlikely candidate for full-scale operation.

3.3 INCORPORATION OF Pd/H_2 SUBMODEL INTO HFTW MODEL

Now that we have developed a submodel for η_{sp}, it must be incorporated into Ferland's (2000) remediation model using HFTW's. This is accomplished by first determining the interflow (I_U and I_L) between the well pair using Christ's (1999) methods. Once these parameters are known, the overall treatment efficiency for the upper and lower aquifer ($\eta_{overallU}$ and $\eta_{overallL}$) is determined using equations (11) and (12), respectively. In order to calculate these efficiencies, we rearrange these equations as seen in equations (23) and (24), respectively:

$$\eta_{overallU} = 1 - \left[\frac{(1-I_L)(1-\eta_{spU}) + I_L(1-I_U)(1-\eta_{spL})(1-\eta_{spU})}{1 - I_U I_L (1-\eta_{spL})(1-\eta_{spU})} \right] \tag{23}$$

$$\eta_{overallL} = 1 - \left[\frac{(1-I_U)(1-\eta_{spL}) + I_U(1-I_L)(1-\eta_{spL})(1-\eta_{spU})}{1 - I_U I_L (1-\eta_{spL})(1-\eta_{spU})} \right] \tag{24}$$

where η_{spU} and η_{spL} represent the single-pass efficiency through treatment reactors in the upflow and downflow treatment wells, respectively. If equal interflow exists in both portions of the aquifer and the single-pass efficiencies are equal for both treatment reactors in the HFTW, equations (23) and (24) simplify to:

$$\eta_{overall} = \frac{\eta_{sp}}{1 - I(1-\eta_{sp})} \tag{25}$$

where $I = I_U = I_L$ and $\eta_{sp} = \eta_{spU} = \eta_{spL}$. For this modeling study, we will assume that pumping rates through all wells in the HFTW system are equal and each well contains equally sized Pd reactors, so that equation (25) applies.

3.4 SENSITIVITY ANALYSIS

Sensitivity analysis (presented in Chapter 4) will begin by examining the submodel presented in this modeling study. The main parameters influencing single-pass efficiency are flow rate (Q), reactor volume (V), and mass loading of contaminant/poison [P]. Adjusting these parameters will allow us to see if submodel simulations are consistent with our conceptual model of how the system should behave. For example, we'd anticipate that increasing the flow rate entering the Pd reactor should result in decreased single-pass efficiency.

Following analysis of the submodel, sensitivity analyses will be performed on the HFTW model incorporating the Pd reactor submodel. In an HFTW system, the main objectives are to ensure the contaminant plume is captured (a minimum CZW is attained) and that contaminant concentrations downgradient of the system meet regulatory requirements, (a minimum $\eta_{overall}$ is achieved). Once these design objectives are known, a design can specify such engineered parameters as flow rate (Q), reactor volume (V), treatment well separation distance ($2d_{half}$), and well pair orientation with respect to the regional groundwater flow direction (α). In an HFTW system, interdependencies exist between these engineering parameters that govern system performance. For example, while increasing the flow rate will increase the CZW and the interflow between wells, overall

system performance may decrease due to a reduced residence time in the reactors. Sensitivity analysis of the HFTW system will be limited to varying the engineering parameters Q, V, and d_{half}.

For analysis purposes, it will be assumed that the upgradient contaminant concentration will be constant throughout the upper and lower portions of the aquifer. As a result, the well pair orientation with respect to the regional groundwater flow direction (α) will be selected such that interflow is equal in the upper and lower portions of the aquifer. This orientation will minimize the single-pass efficiency for both reactors needed to obtain a specified overall treatment in both the lower and upper aquifer. Figure 3.3 plots α corresponding to equal interflows in the upper and lower portions of the aquifer based on B_U/B_L and V_{col}/V_{gw}, where B_U and B_L are the widths of the upper and lower portions

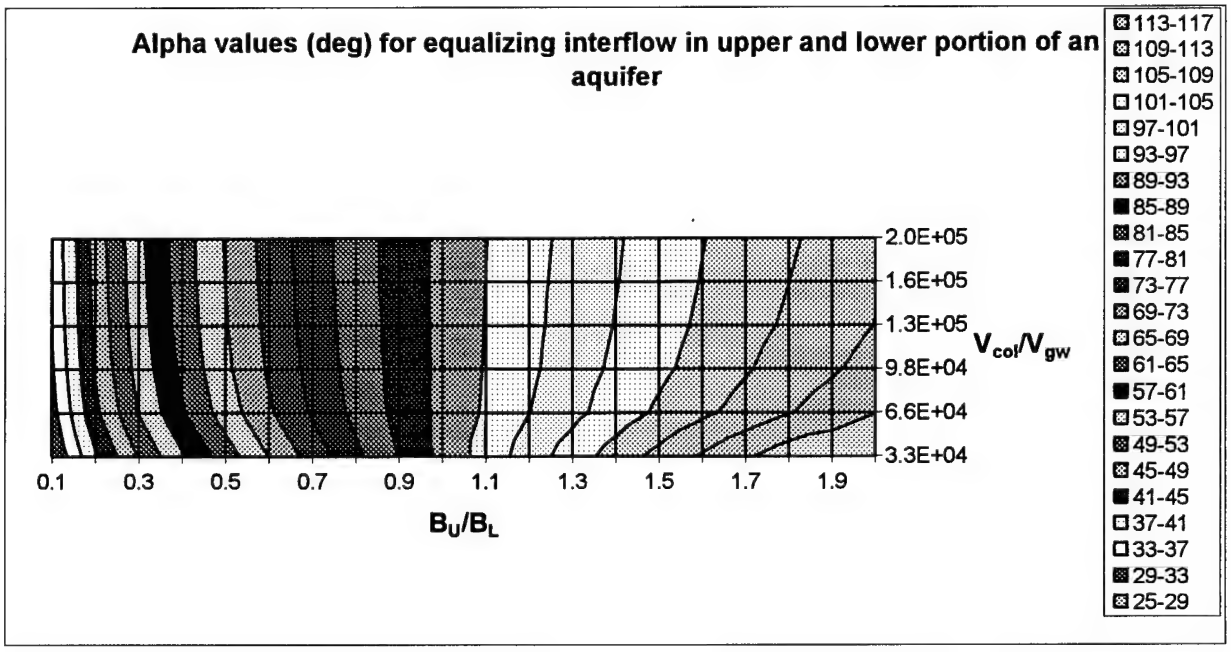

Figure 3.3 Alpha values that equalize interflow for various B_U/B_L and V_{col}/V_{gw} (A = 0.018 m^2, d_{half} = 8 m)

of the aquifer, respectively, and V_{col} and V_{gw} represent the column and regional groundwater flow velocities (where $V_{col} = Q/nA$ and A is the cross-sectional area of the reactor), respectively. As an example, consider a hypothetical scenario of an upper and lower aquifer width of 4 and 9 m, respectively, a groundwater flow velocity (V_{gw}) of 0.02 m/d, and a column velocity (V_{col}) of 80 cm/min. Using Figure 3.3, we see that an alpha value of approximately 59 degrees will equalize the interflow in both portions of the aquifer. Note that Figure 3.3 was constructed using a specific column cross-sectional area (A) of 0.018 m^2 and a d_{half} value of 8 m. For different column cross-sectional areas and half-distances between treatment wells, different figures must be constructed.

3.5 MODEL VERIFICATION

Following the sensitivity analysis, the reactor submodel will be tested by comparing simulation results of single-pass efficiency to experimental data using contaminated groundwater from Moffett Field, CA (Lowry and Reinhard, 2000a). The HFTW model and Figure 3.3 will then be applied to remediate a hypothetical contaminated groundwater plume based on aquifer conditions at Edwards AFB, CA. For this hypothetical plume, the performance predictions from this model and Ferland's (2000) model will be compared and discussed.

4.0 ANALYSIS

4.1 INTRODUCTION

In this chapter, we analyze the model developed in Chapter 3. The chapter begins with sensitivity analyses of the Pd reactor submodel and HFTW model. Submodel verification will be performed by comparing simulation output to experimental column results (Lowry and Reinhard, 2000a). In the final portion of the chapter, we compare performance predictions of the model developed in this study with predictions of Ferland's (2000) remediation model.

4.2 SENSITIVITY ANALYSIS

4.2.1 REACTOR SUBMODEL

Single-pass efficiency is a function of the residence time and catalyst deactivation. The rate of catalyst deactivation depends on the deactivation rate constant, which in turn is dependent on the particular contaminant/poison mass loading passing through the Pd reactor and the mass of catalyst used. For a given influent contaminant/poison concentration, proportionally increasing both the reactor volume and flow rate (such that the residence time remains constant) will not affect the rate at which catalyst deactivation occurs. The increased contaminant/poison loading through the column that is a result of increased flow doesn't speed catalyst deactivation because the increased reactor volume contains a proportionally larger mass of catalyst. In order to see the effect of catalyst mass on catalyst deactivation, we run submodel simulations for reactors with equal residence times and mass (contaminant/poison) loadings, but with different catalyst masses. In Figure 4.1, we compare two flow rates (1 and 2 mL/min) through two

different columns (both 1.27 cm diameter, but one column is 7 cm long, the other 14 cm long). For the remainder of the analysis in this section, all columns will be assumed to have a diameter of 1.27 cm. In addition, the calibrated k_{obs0} value of 1.25 min^{-1} (Figure 3.1) will be used for the remainder of the analysis. Note that the residence time in both columns in Figure 4.1 is the same (3.7 min).

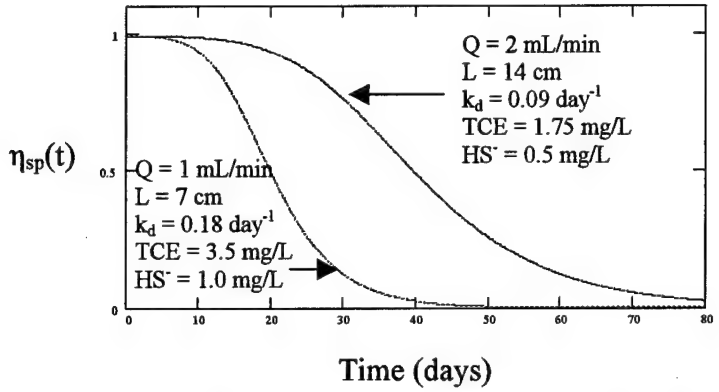

Figure 4.1 Effect of increasing g_{cat} for equal mass contaminant/poison loading (4.5 mg poison/contaminant min^{-1}), residence time (3.7 min)

As anticipated, the model shows that for the same mass loading of contaminant/poison entering the reactor, increasing the catalyst mass results in decreasing the rate of catalyst deactivation. Note this effect is due to equation (20). As g_{cat} increases, the deactivation rate constant (k_d) decreases, resulting in slower catalyst deactivation.

In Figure 4.2, we illustrate the effect of varying residence time (t_r) on single-pass efficiency (η_{sp}) using an influent TCE and HS^- concentration of 3.5 and 1.0 mg/L, respectively. In Figure 4.2a, the residence time is increased in a 7 cm column from 1.9 to 3.7 minutes by decreasing the flow rate from 2 to 1 ml/min. As expected, the larger residence time results in higher single-pass efficiencies. The lower flow rate (1 mL/min)

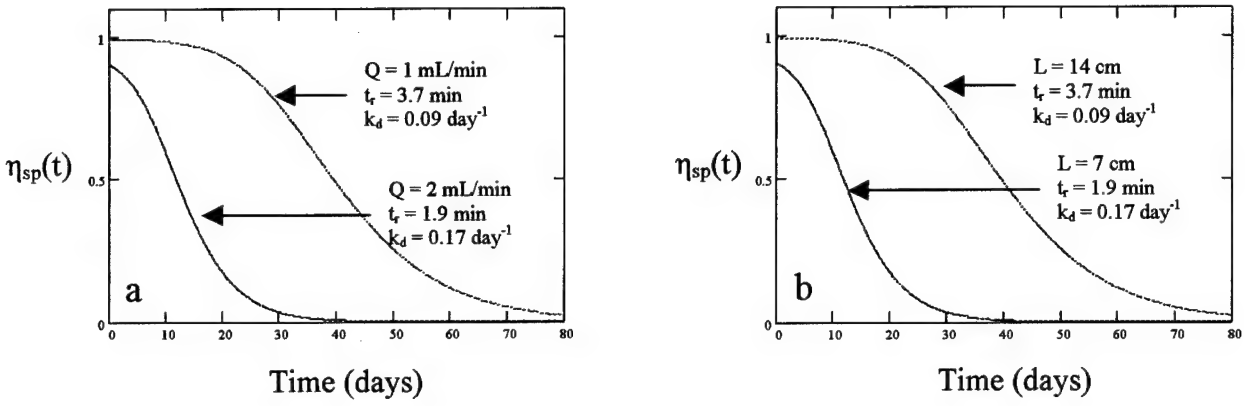

Figure 4.2 Effect of increasing residence time on single-pass- efficiency by a) decreasing flow rate (Q) and b) increasing column length (L)

also decreases the mass loading, resulting in a smaller k_d value and less rapid deactivation. Figure 4.2b illustrates the effect of increasing the residence time (from 1.9 to 3.7 min) by doubling the column length (7 to 14 cm) and holding the flow rate constant (2 mL/min). Once again, the larger residence time results in higher single-pass efficiencies. The smaller value of k_d is the result of more catalyst mass in the longer column. Note that the initial single-pass efficiency at T = 0 calculated by the submodel is solely a function of the residence time (t_r) and the first-order rate constant (k_{obs0}). As time progresses, single-pass efficiency decreases due to catalyst deactivation.

Figure 4.3 illustrates the effect of injecting additional poison (20 mg/L SO_3^{2-}) into the column using the same column length (7cm), and TCE and HS^- influent concentrations (3.5 and 1.0 mg/L, respectively) used in Figure 4.2a. The single-pass efficiencies observed at the beginning of the simulation are equal, indicating that catalyst poisons do not affect initial efficiency. The catalyst deactivates with time and we see that the

simulation with 20 mg/L SO_3^{2-} shows faster decreases in single-pass efficiency (due to a relatively larger k_d value).

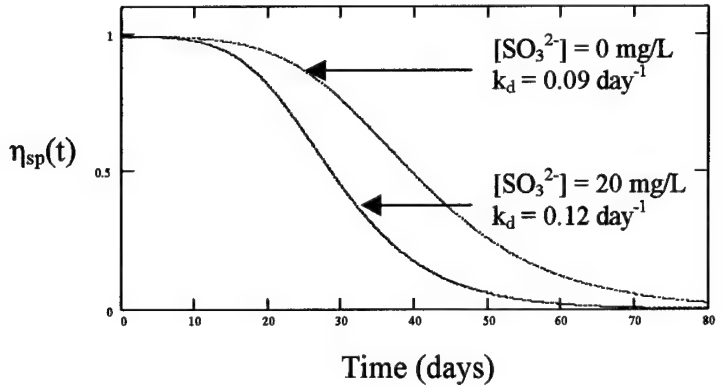

Figure 4.3 Effect of injecting additional poison (SO_3^{2-}) on single-pass efficiency (Q = 1 mL/min)

Non-dimensionalizing our parameters, Figure 4.4 displays the single-pass efficiency for different non-dimensional residence times (t_r*k_{obs0}) and non-dimensional reactor operating times ($T*k_d$). In general, higher single-pass efficiencies are attained in the upper left quadrant ($t_r*k_{obs0} >> T*k_d$). Efficiency decreases as non-dimensional reactor operating time increases and/or non-dimensional residence time decreases.

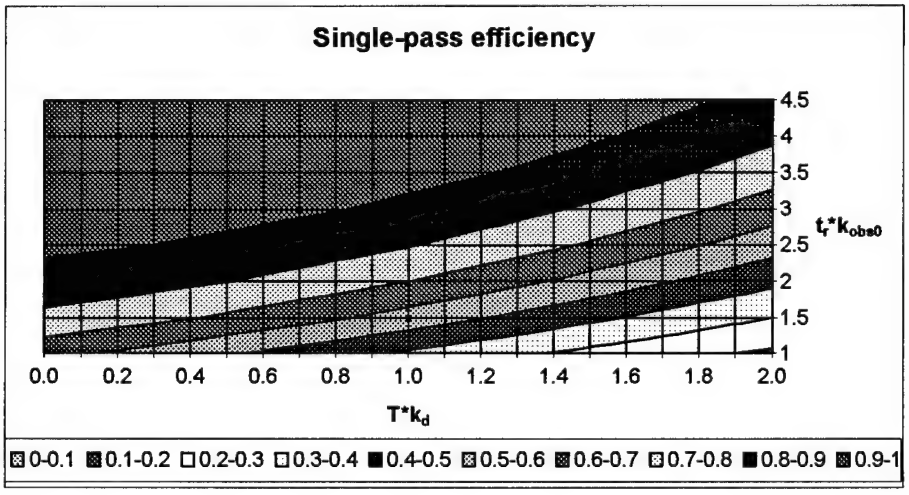

Figure 4.4 Single-pass efficiency (η_{sp}) as a function of non-dimensional operating time ($T* k_d$) and non-dimensional residence time ($t_r *k_{obs0}$)

Consider a scenario with the following column parameters: column length = 14 cm, k_d = 0.10 day^{-1} (comprised of influent concentrations of [TCE] = 3.5 mg/L, $[HS^-]$ = 0.8 mg/L, and flow rate = 3.0 mL/min), and t_r = 2.5 min. In order to determine the single-pass efficiency after 10 days operation, calculate the non-dimensional operating and residence times (1.03 and 3.13, respectively). The reader can see in the following magnified view of Figure 4.4 that the single-pass efficiency for these non-dimensional times is approximately 88%.

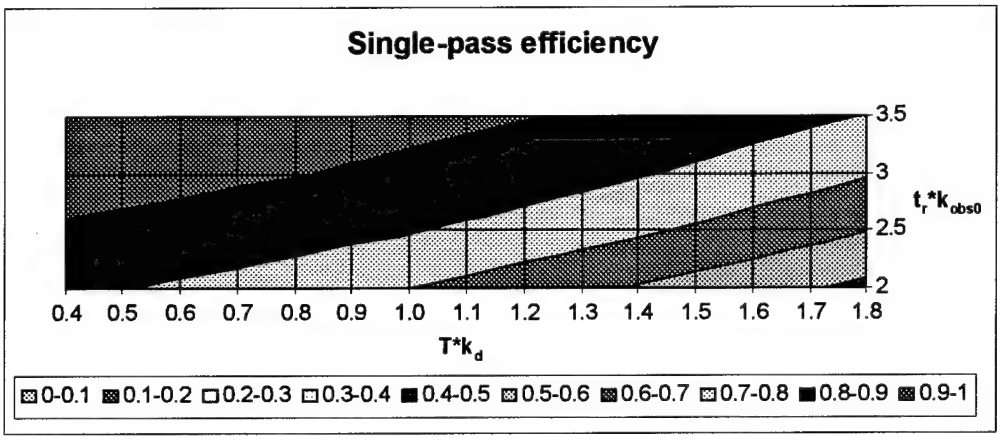

Figure 4.5 Magnified view of Figure 4.4

4.3 MODEL PREDICTIONS COMPARED TO EXPERIMENTAL RESULTS

In this section, we apply the submodel to experimental column results (Lowry and Reinhard, 2000a) in two examples. The first column experiment was performed to investigate the effects of HS^- and regeneration by sodium hypochlorite in deionized water ($[TCE]_{in}$ = 3.5 mg/L) using a 0.56 cm column (0.5 gm Pd/Al catalyst) and a flow rate of 1 mL/min. Figure 4.6 plots simulation results and experimental results (Lowry and Reinhard, 2000a).

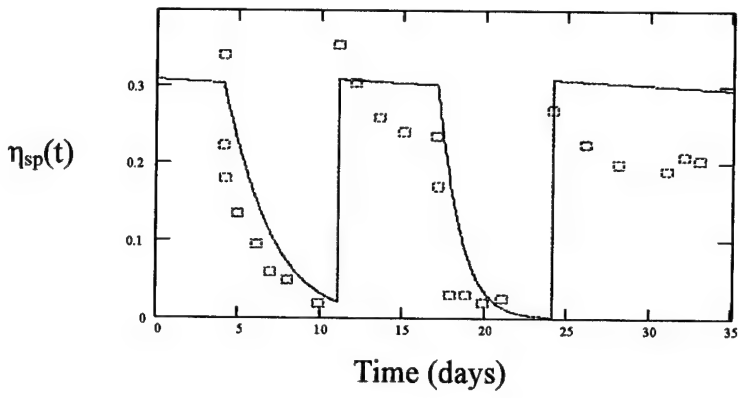

Figure 4.6 Submodel output compared to experimental column results (Figure 5b, Lowry and Reinhard (2000a))

At T = 4 days, 0.4 mg/L HS^- was continuously injected into the column (Q = 1 mL/min) until the first regeneration was accomplished at T = 11 days. HS^- (0.8 mg/L) was injected a second time between days 17 and 24, prior to the second regeneration. While submodel output reasonably agrees with experimental results during the periods of injecting HS^- into the column and regeneration, the greatest variation is found directly following regeneration (days 11 and 24). At 11 days, we see the submodel slightly underestimates the effectiveness of regeneration. Subsequently, the submodel underestimates the rate of decline in treatment efficiency prior to the next injection of HS^-. At the second regeneration, or day 24, the submodel slightly overestimates the effectiveness of regeneration and thereupon underestimates the rate of decline in treatment efficiency. The submodel's underestimation of the rate of decline in treatment efficiency, after both regenerations may be due to residual HS^- that remains on the catalyst surface after each regeneration. The poison, which is not accounted for in the submodel, may lend to deactivation being more rapid than expected. The reader will note that the difference between submodel output and experimental results between days 11 - 17 (HS^- = 0.4 mg/L) is less than the difference between days 17 – 24 (HS^- = 0.8 mg/L).

The second column experiment was performed to ascertain the catalyst's ability to destroy TCE using actual groundwater from Moffett Field rather than DI water. The parameters used in this experiment (Q, g_{cat}, TCE_{in}) were the same as those used in the previous example. Figure 4.7 compares submodel output with experimental results (Lowry and Reinhard, 2000a). After 20 days operation, 0.1 ± 0.05 mg/L HS^- was detected in the column effluent. The authors speculate this may have resulted from the growth of sulfate reducing bacteria that thrived on the ample supply of aqueous hydrogen

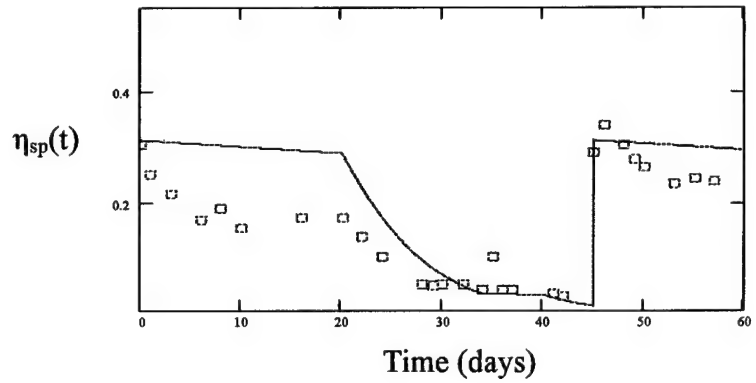

Figure 4.7 Submodel output compared to experimental column results using Moffett groundwater (Figure 6a, Lowry and Reinhard (2000a))

(electron donor) and sulfate (177 mg/L) within the column (Lowry and Reinhard 2000a). At T = 34 days, a regeneration was performed using a dilute hypochlorite solution (75 mg/L). Although the regeneration only resulted in a slight increase in treatment efficiency, the hypochlorite obviously had an impact on sulfate reduction, as HS^- was not detected in the column effluent until six days later. The second regeneration (750 mg/L) was performed at 45 days and resulted in significantly higher contaminant destruction efficiencies. This suggests the extent to which catalyst sites are recovered during regeneration is dependent on the concentration of the regenerant.

Referring to the submodel simulation in Figure 4.7, we see that TCE destruction is notably lower than the submodel prediction during the first 20 days operation. This may be due to deactivation of the catalyst by inorganic species not accounted for in the submodel. During the first 20 days, the submodel only accounted for TCE (3.5 mg/L). At T = 20 days, HS^- at 0.15 mg/L was added to the influent. The upper bound of the measured concentration range is used since it is reasonable to assume that the HS^- concentration actually within the column may be greater than the effluent concentration. Since the first regeneration results in minimal efficiency increases, we simulate this time period as if no regeneration had occurred. However, we speculate that the regeneration reduced the formation of HS^-, so for days 34 – 40 the submodel assumes $HS^- = 0$ mg/L. The reappearance of HS^- is modeled by introducing 0.15 mg/L HS^- from day 40 until the second regeneration (day 45). Finally, at T = 45 days, the submodel simulates regeneration occurs and HS^- is reset to 0 mg/L. Based on Figure 4.7, it appears the submodel reasonably adequate job of qualitatively predicting contaminant destruction in a Pd/H_2 column.

4.4 HFTW SYSTEM (2 WELLS)

In the HFTW system, overall treatment efficiency ($\eta_{overall}$) is dependent on the single-pass treatment efficiency (η_{sp}) and interflow (I_L and I_U) between upflow and downflow treatment wells. In addition to these parameters, a system designer must also consider the CZW required to contain a contaminant plume. Before going any further, it may be helpful to list the factors that influence these important design parameters (η_{sp}, $\eta_{overall}$, I_U (and I_L), and CZW).

Parameter	Factors influencing parameter	Equations
η_{sp}	t_r (V/Q), contaminant/poison conc.	20
$\eta_{overall}$	I_U, I_L, η_{sp}	23, 24
$I_U(I_L)$	Q, U, B, α, d_{half}	Christ (1997)
CZW	Q, $I_U(I_L)$	Ferland (2000) and Christ (1997)

Table 4.1 Engineering parameters affecting HFTW treatment efficiency

As mentioned in Chapter 3, this modeling study does not examine the effect of varying α on overall treatment efficiency. However, it is interesting to consider the effect of the well pair orientation on catalyst deactivation. For α values other than 90 deg, we might suspect the upgradient treatment well deactivates sooner than the downflow treatment well due to a relatively larger contaminant/poison loading. However, we will assume that only a negligible portion of the influent poison mass passing through the catalyst column is able to deactivate the catalyst. Therefore, the contaminant/poison mass loading for the upgradient and downgradient treatment wells is relatively equal, resulting in equal k_d values for both treatment reactors. Catalyst deactivation observed during column experiments using Moffett Field groundwater (Lowry and Reinhard, 2000a) resulted in a detection of HS^- (0.1 mg/L) in the column effluent, which supports the notion that only a relatively small mass of poison results in noticeable catalyst deactivation.

4.4.1 FLOW RATE

Our sensitivity analysis of the HFTW system begins by assuming equal upper (B_u) and lower (B_L) aquifer depths and that the well pair orientation is perpendicular to the regional groundwater flow direction (α = 90 deg). This results in equal interflow in both portions of the aquifer ($I_U = I_L$), so $C_{outU} = C_{outL}$ (since upflow and downflow treatment

wells are identically configured). Table 4.2 lists the HFTW operating parameters and regional aquifer characteristics used for this sensitivity analysis. In addition to increasing the reactor volume to a size more appropriate for with field-scale operations, we assume that sulfate is reduced to HS^- due to the growth of sulfate-reducing microorganisms in the catalyst column. Therefore, a HS^- concentration of 0.6 mg/L is entered into the submodel to simulate catalyst poisoning due to sulfate reduction.

HFTW configuration	
Pumping rate	10 L/min
Column length	2.5 m
Column diameter	15 cm
Half-distance between wells	10 m

Aquifer characteristics	
Groundwater flow velocity	0.02056 m/d
Aquifer width ($B_U = B_L$)	8m
TCE	3.5 mg/L
SO_4^{2-}	170 mg/L

Table 4.2 HFTW operating parameters and regional aquifer characteristics

Figure 4.8 illustrates the effect of increasing the pumping rate by 100%. While interflow and the CZW is increased, overall treatment efficiency decreases as a result of decreasing

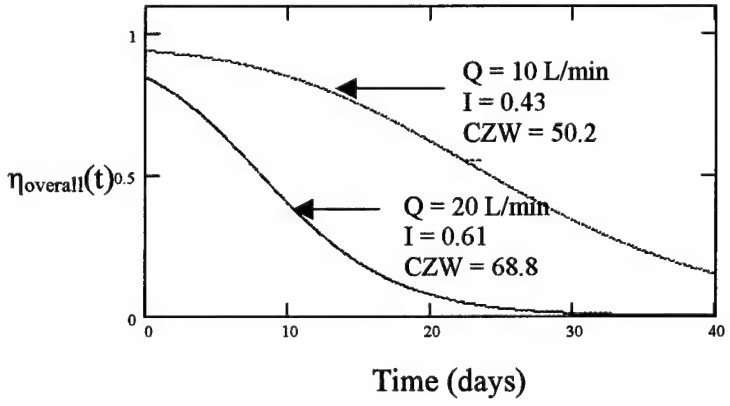

Figure 4.8 Effect of increasing pumping rate on HFTW efficiency ($\eta_{overall}$)

the single-pass efficiency (lower residence time). In addition, increasing the pumping rate produces a greater mass contaminant/poison loading through the column. This

results in a larger k_d value leading to a more rapid rate of decreased treatment efficiency (larger k_d).

4.4.2 WELL SEPARATION DISTANCE

Figure 4.9 illustrates the effect of increasing interflow by reducing the well separation half distance by 40% (from 10 m to 6 m). System performance is slightly improved at the expense of decreasing the CZW. Looking at Figures 4.8 and 4.9, we can make a few statements about the HFTW system. First, high system performance is more dependent

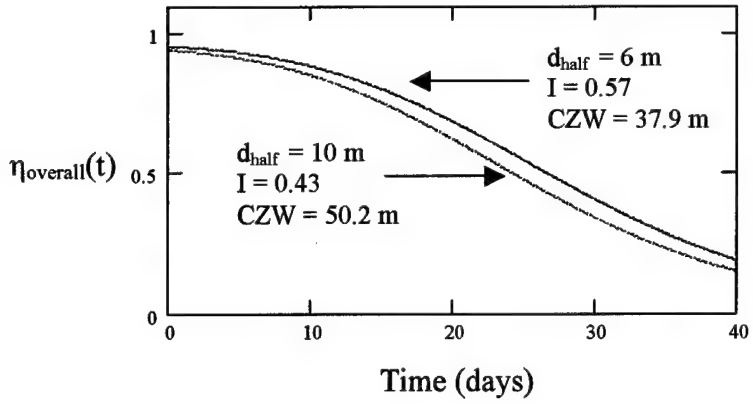

Figure 4.9 Effect of decreasing the well separation distance on HFTW efficiency

on single-pass efficiency than the interflow between treatment wells. Second, increasing the pumping rate to achieve a higher CZW reduces the overall treatment efficiency due to decreased single-pass efficiency. As a result, larger treatment reactors are needed to offset the decrease in residence time. Third, increasing the pumping rate deactivates the catalyst at a greater rate (due to increased mass loading of contaminant/poison through the column), resulting in more frequent regenerations. Table 4.3 lists the variables influenced by the pumping rate and well separation distance and how they relate to one another. A plus sign indicates a positive relationship (e.g. as Q increases, the catalyst

deactivation rate (k_d) increases) and a negative sign indicates a negative relationship (e.g. as d_{half} decreases, HFTW system efficiency ($\eta_{overall}$) increases).

Q	Parameters influenced by Q and d_{half}	d_{half}
+	Capture zone width (CZW)	+
-	Single-pass efficiency (η_{sp})	ne
-	HFTW system efficiency ($\eta_{overall}$)	-
+	catalyst deactivation rate (k_d)	+
+	Interflow ($I_{U,L}$)	-

ne - indicates parameter has no effect on $\eta_{sp}(t)$

Table 4.3 Parameters affected by pumping rate (Q) and well separation distance (d_{half})

Note that the well separation distance does not affect the single-pass efficiency. This is due to the assumption that only a relatively small portion of the influent poison mass deactivates the catalyst. Therefore, changing interflow will not affect the amount of poison entering the catalyst column, which allows us to use equal k_d values for both treatment reactors.

As mentioned in Chapter 2 (Figure 2.5), Ferland (2000) constructed HFTW efficiency contour graphs by plotting the non-dimensional flow rate (Q/UBd) against the non-dimensionalized residence time ($k_{obs0}t_r$). In order to account for decreased system performance due to catalyst deactivation, multiple contour diagrams are constructed at various times (T) using a single deactivation rate constant (k_d) value equal to 0.1 day^{-1}. Figure 4.10 illustrates four HFTW efficiency contour plots at T = 5, 10, 20, and 30 days, respectively. Assuming the upper and lower portions of the aquifer are equal in width allows us to generate one efficiency plot for the entire aquifer. The reader will note that for small values of non-dimensionalized flow rate, the contours are relatively flat. This region represents 0 interflow between treatment wells and HFTW efficiency is equal to

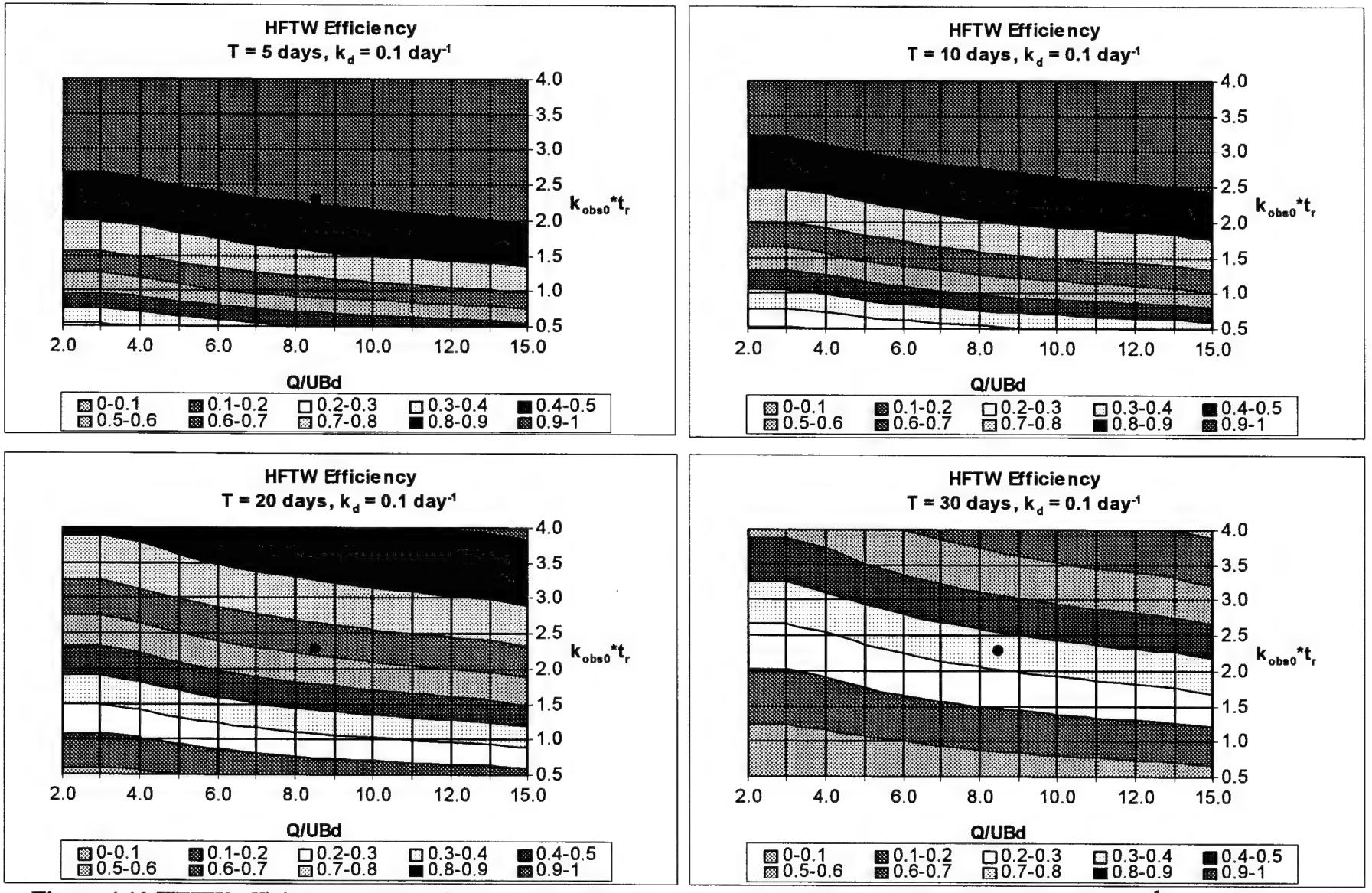

Figure 4.10 HFTW efficiency contour plots at T = 5, 10, 15, 20 days (α = 90 deg, $B_U = B_L$ = 8 m, k_d = 0.1 day^{-1})

the single-pass efficiency. As we increase the flow (but holding the residence time constant by increasing the column length), the contours begin to slope downward, indicating higher system performance is achieved with increasing flow due to increased interflow.

We again refer to the hypothetical HFTW operating parameters listed in Table 4.2 to demonstrate the usefulness of Figure 4.9. The k_d value for this configuration is 0.1 day^{-1}, matching the k_d value used to construct Figure 4.10. Calculating the non-dimensionalized pumping rate and residence time, we get 8.49 and 2.39, respectively. These operating parameters correspond to the following system efficiencies (at T = 5, 10, 20, and 30 days, respectively): 91%, 86%, 65%, and 37%. Figure 4.11 shows the decrease in overall HFTW efficiency over time for the aforementioned engineering parameters.

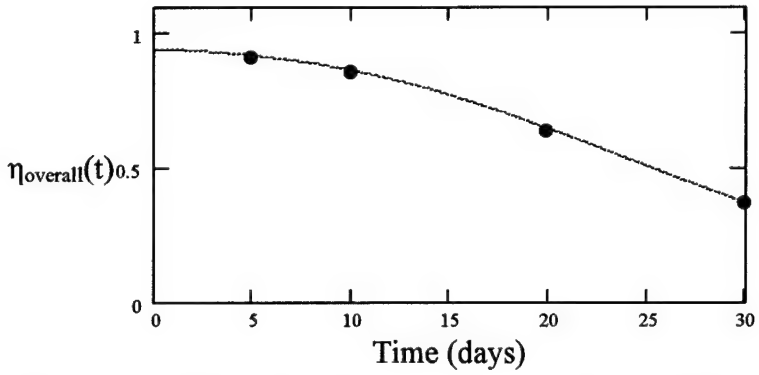

Figure 4.11 Overall efficiency vs time for HFTW system operation using Table 4.2 parameters

4.5 GENERAL APPLICATION TO HYPOTHETICAL SITE

In this section, we apply the HFTW model with the Pd reactor submodel to simulate remediation of a hypothetical contaminated groundwater site. In order to compare model

predictions between the model developed in this thesis and Ferland's (2000) HFTW remediation model, we will use the same scenario used in Ferland's (2000) thesis. Table 4.4 lists site characteristics and HFTW engineering parameters used by Ferland (2000).

Aquifer condtions (Edwards AFB)	
Darcy velocity	.02056 m/d
B_U	8 m
B_L	5 m
TCE	15 mg/L
SO_4^{2-}	170 mg/L
Plume Width	200 m

HFTW enginering parameters	
Q	45 m^3/d
d_{half}	40 m
α (upper aquifer)	67.5 deg
column length	36 m
column diameter	15.24 cm

Table 4.4 Hypothetical scenario conditions (taken from Edwards AFB)

Note this scenario also incorporates the presence of sulfate in the groundwater. A value of 0.6 mg/L HS^- will be assumed in the catalyst column due to the presence of sulfate reducing microorganisms.

4.5.1 MODEL COMPARISON

Figure 4.12 illustrates overall HFTW system efficiency in the upper aquifer using Ferland's (2000) model and the model developed in this thesis. As expected, system performance predictions from both models initially are equal. As time progresses, catalyst deactivation results in decreasing overall efficiency predictions by the model in

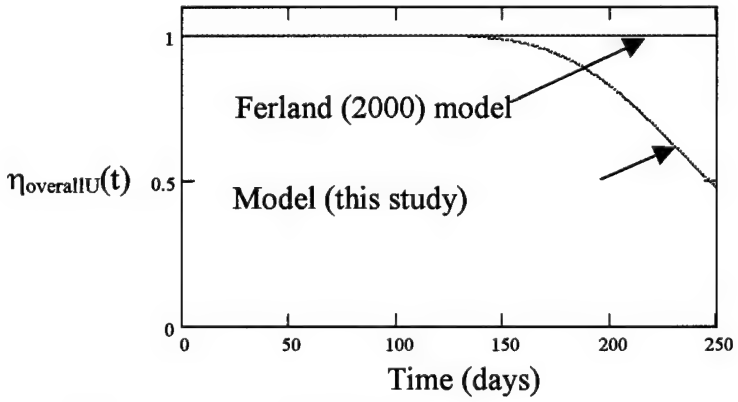

Figure 4.12 Comparison of HFTW models

this thesis, while the Ferland (2000) model predicts no performance decreases. Note that for the parameters used in this hypothetical, though realistic, scenario, significant catalyst deactivation is not observed until approximately 130 days into the simulation. For an HFTW system operating using the engineering parameters in Table 4.4, it appears that catalyst deactivation may not be an important cost factor, as the cost of regeneration every four months would not significantly impact cost. Note, however, that a column length of 36 m may not be practical in many cases. The above design, however, uses only two treatment wells to capture a 200 m wide plume and attain downgradient TCE concentrations of < 5ppb. In fact, multiple well pairs could be used. For example, incorporating an additional well pair would reduce the required pumping rate of a single well and the in-well reactor size by a factor of two without changing the original residence time. The deactivation rate constant (k_d) also remains constant since the ratio of contaminant/poison loading to the amount of catalyst used in a treatment well remains constant.

5.0 CONCLUSIONS

5.1 SUMMARY

In this thesis, a submodel describing the palladium catalyzed destruction of chlorinated ethenes was presented. Using experimental column results (Lowry and Reinhard, 2000a), catalyst deactivation was modeled by replacing the observed first-order rate constant (k_{obs0}) with a time dependent rate constant ($k_{obs}(t)$). The rate at which $k_{obs}(t)$ is reduced due to deactivation depends on the contaminant/poison mass loading and the amount of catalyst used. Regeneration was modeled as an instantaneous process that restored catalyst treatment efficiency to the efficiency observed at the beginning of system operation. The submodel was then incorporated into Ferland's (2000) HFTW flow model. Non-dimensional contour plots describing single-pass and overall efficiency were constructed using the combined catalyst and HFTW model. In addition, the combined model was used to simulate overall treatment efficiency at a contaminated site.

5.2 CONCLUSIONS

- **Catalyst deactivation can be incorporated into a first-order model by modeling the first-order rate constant as a function of time.** The submodel was able to qualitatively predict the effect of catalyst poisoning on contaminant destruction. Model overestimation of destruction efficiency following regeneration compared to experimental results (Lowry and Reinhard, 2000a) appears due to the submodel's assumption of complete regeneration and the presence of additional catalyst poisons that are unaccounted for in the submodel.

- **Changes in flow through the treatment wells have a greater influence on system performance in the HFTW system than changes to the well separation distance.** Sensitivity analyses revealed a greater impact on system performance by varying the flow rate than by comparable changes in the well separation distance. This is expected since varying the flow rate affects the residence time in the in-well reactor and the interflow between the well pair, both of which contribute to overall treatment efficiency. Varying the well separation distance only affects the interflow and therefore has a lesser impact on overall treatment efficiency.

- **The submodel qualitatively describes treatment efficiency observed in a laboratory column treating contaminated groundwater using the Pd/H_2 system.** Based on the treatment system operating parameters and aquifer geochemistry, the model qualitatively predicted treatment efficiency decline over time, as well as the effect of regeneration, in a laboratory experimental column treating groundwater from Moffett Field.

- **Applying the model in this study to a realistic contaminated aquifer scenario using HFTW parameter values showed that insignificant catalyst deactivation would be anticipated over approximately 130 days of HFTW operation.** It therefore appears that catalyst deactivation may not be an important cost factor, as the cost of regeneration every four months would not significantly impact cost.

- **This model, by incorporating the relevant processes of catalyst deactivation and regeneration, represents an important step in transitioning the Pd/H_2 in-well system to field application.** The submodel presented in this study and validated by experimental data, coupled with the HFTW flow model, allows developers to predict field-scale technology performance.

5.3 RECOMMENDATIONS

- **Investigate the effect of multiple catalyst poisons on catalyst destruction efficiency**. The deactivation rate constant was calculated as the sum of the k_d values of the individual constituents contributing to catalyst deactivation. This assumes that a poison's affinity for the catalyst surface remains constant regardless of the total number of poisons entering the catalyst column. This assumption should be experimentally tested.

- **Incorporate Pd reactor submodel into other groundwater flow models.** The simplifications of Ferland's (2000) analytical groundwater flow model are adequate for use as an initial screening tool. However, incorporation of the submodel into a more realistic numerical flow model will allow us to better simulate field-scale operations.

- **Perform additional column experiments to determine deactivation rate constant (k_d) values for other suspected catalyst poisons.** Although any number of poisons can be modeled using the submodel presented in this study, the only values of k_d

currently available are for TCE, HS^-, and SO_3^{2-} as species contributing to catalyst deactivation. Column experiments using contaminated groundwater from Moffett Field provide evidence that other sources (inorganic or biological) contribute to catalyst deactivation. Since the submodel initially overestimated contaminant destruction using groundwater from Moffett Field, it is likely that other groundwater constituents contribute to catalyst deactivation. Further research is needed to identify other potential catalyst poisons (inorganic and biological).

- **Develop a model for daughter product distribution.** The production of vinyl chloride (VC) and its detection in the effluent is a major concern for any remediation strategy involving the reduction of chlorinated ethenes. As catalyst deactivation occurs, the probability of VC breakthrough increases. The model presented in this study does not include production of daughter products. Incorporation of daughter product production into the model will further enhance the usefulness of the model—allowing us to predict the presence of potentially harmful compounds such as VC in the reactor.

- **Validate the combined HFTW and in-well Pd/H_2 reactor models.** A field-scale evaluation of the HFTW technology with in-well Pd/H_2 reactors is planned at Edwards AFB in the coming year. Data from this evaluation may be used to validate model predictions.

BIBLIOGRAPHY

Boggs, K. A., Bench-Scale Investigation of Catalytic Dehalogenation of Chlorinated Ethenes with Palladium Metal. MS Thesis, Wright-State University, July 2000.

Chang, C. C., C. M. Reo, and C. R. F. Lund, "The Effect of a Membrane Reactor upon Catalyst Deactivation During Hydrodechlorination of Dichloroethane," Applied Catalysis B: Environmental, 20(4): 309-317, 1999.

Christ, J. A., A Modeling Study for the Implementation of In Situ Cometabolic Bioremediation of Trichloroethylene-Contaminated Groundwater. MS Thesis, AFIT/GEE/ENV/97D-03. School of Engineering and Environmental Management, Air Force Institute of Technology, (AU), Wright-Patterson AFB OH, December 1997.

Christ, J. A., M. N. Goltz, and J. Huang, "Development and Application of an Analytical Model to Aid Design and Implementation of In Situ Remediation Technologies," Journal of Contaminant Hydrology, 37(3): 295-317, 1999.

Clark, M. M., Transport Modeling for Environmental Engineers and Scientists. New York: John Wiley and Sons, 1996.

Daub, K., G. Emig, M. J. Chollier, M. Callant, and R. Dittmeyer, "Studies on the Use of Catalytic Membranes for Reduction of Nitrate in Drinking Water," Chemical Engineering Science, 54(10): 577-1582, 1999.

Defense Environmental Restoration Program (DERP), Fiscal Year 1998 Annual Report to Congress, Washington: Government Printing Office, 1999.

Domenico, P. A., and F. W. Schwartz, Physical and Chemical Hydrogeology, New York: John Wiley & Sons, Inc., 1998.

Ferland, D. R., In Situ Treatment of Chlorinated Ethene-Contaminated Groundwater Using Horizontal Flow Treatment Wells. MS Thesis, AFIT/GEE/ENV/00M-05, 1999. School of Engineering and Environmental Management, Air Force Institute of Technology, (AU), Wright-Patterson AFB OH, December 1999.

Gu, B., T. J. Phelps, L. Liang, M. J. Dickey, Y. Roh, B. L. Kinsall, A. V. Palumbo, and G. K. Jacobs, "Biogeochemical Dynamics in Zero-Valent Iron Columns: Implications for Permeable Reactive Barriers," Environmental Science and Technology, 33(13): 2170-2177, 1999.

Kovenklioglu, S., Z. Cao, D. Shah, R. J. Farrauto, and E. N. Balko, "Direct Catalytic Hydrodechlorination of Toxic Organics in Wastewater," AIChE Journal, 38(7): 1003-1012, 1992.

Kramer, H., M. Levy, and A. Warshawsky, "Hydrogen Storage by the Bicarbonate/Formate Reaction. Studies on the Activity of Pd Catalysts," International Journal of Hydrogen Energy, 20(3): 229, 1995.

Levenspiel, O., Chemical Reaction Engineering, 3rd Edition. New York: John Wiley and Sons, 1999.

Lowry, G. V., Palladium-catalyzed TCE Dechlorination in Groundwater: Dechlorination Kinetics, Dissolved Solute Effects, and Catalyst Regeneration. Ph.D Dissertation. Stanford University, August 2000.

Lowry, G. V. and M. Reinhard, "Pd-Catalyzed TCE Dechlorination in Groundwater: Solute Effects, Biological Control, and Oxidative Catalyst Regeneration," Environmental Science and Technology 34(15): 3217-3223, 2000.

Lowry, G. V. and M. Reinhard, "Pd-Catalyzed TCE Dechlorination in Water: Effect of $[H_2]_{(aq)}$ and H_2 Utilizing Competitive Solutes on the TCE Dechlorination Rate and Product Distribution," Environmental Science and Technology (submitted in 2000).

Lowry, G. V. and M. Reinhard, "Hydrodehalogenation of 1- to 3- Carbon Halogenated Organic Compounds in Water Using a Palladium Catalyst and Hydrogen Gas," Environmental Science and Technology, 33(11): 1905-1910, 1999.

Masters, G. R., Introduction to Environmental Engineering and Science, Second Edition. Upper Saddle River: Prentice-Hall, Inc., 1997.

McCarty, P. L., M. N. Goltz, G. D. Hopkins, M. E. Dolan, J. P. Allan, B. T. Kawakami, and T. J. Carrothers, "Full-Scale Evaluation of In Situ Cometabolic Degradation of Trichloroethylene in Groundwater through Toluene Injection," Environmental Science and Technology, 32(1): 88-100, 1998.

McMahon, P. B., K. F. Dennehy, and M. W. Sandstrom, "Hydraulic and Geochemical Performance of a Permeable Reactive Barrier Containing Zero-Valent Iron," Denver Federal Center, Ground Water, 37(3): 396-404, 1999.

McNab, W. W. and R. Ruiz, "Palladium-Catalyzed Reductive Dehalogenation of Dissolved Chlorinated Aliphatics Using Electrolytically-Generated Hydrogen," Chemosphere, (37)5: 925-936, 1998.

McNab, W. W., and R. Ruiz, "In-Situ Destruction of Chlorinated Hydrocarbons in Groundwater Using Catalytic Reductive Dehalogenation in a Reactive Well: Testing and Operational Experiences," Environmental Science and Technology, 34(1): 149-153, 2000.

Munakata, N. "Surface Chemistry of Pd-Catalyzed Hydrodehalogenation: Preliminary Results with Model and PMC Dispersed Catalysts," Hazardous Substance Research Centers Research Symposium, Asilomas Conference Grounds, CA, 9-12 July 2000.

Munakata, N., P. V. Roberts, M. Reinhard, and W. W. McNab, "Catalytic Dechlorination of Halogenated Hydrocarbon Compounds Using Supported Palladium: A Preliminary Assessment of Matrix Effects," Groundwater Quality, 250: 491-496: 1998.

O'Hannesin, S. F. and R. W. Gillham, "Long-Term Performance of an In Situ 'Iron Wall' for Remediation of VOCs," Groundwater, 36(1): 164-180, 1998.

National Research Council, Alternatives for Ground Water Cleanup. Washington: National Academy Press, 1994.

Office of Solid Waste and Emergency Response (OSWER). Directive 9200.4-17P, 1999

Pintar, A., J. Batista, J. Levec, and T. Kajiuchi, "Kinetics of the Catalytic Liquid-Phase Hydrogenation of Aqueous Nitrate Solutions," Applied Catalysis B: Environmental 11(1): 81-98, 1996.

Rylander, P. N. Catalytic Hydrogenation in Organic Syntheses. New York: Academic Press, 1979.

Schreier, C. G. and M. Reinhard, "Catalytic Hydrodehalogenation of Chlorinated Ethylenes Using Palladium and Hydrogen for the Treatment of Contaminated Water," Chemosphere, 31(6): 3475-3487, 1995.

Schüth C., S. Disser, F. Schüth, and M. Reinhard, "Hydrodechlorination and Hydrogenation of Aromatic Compounds over Palladium on Alumina in Hydrogen-Saturated Water," Applied Catalysis B: Environmental (18): 215-222, 1998.

Starr, R. C., and J. A. Cherry, "In Situ Remediation of Contaminated Groundwater: The Funnel-and-Gate System," Ground Water, 32(3): 465-476, 1994.

Thomas, J. M. and W. J. Thomas. Principles and Practice of Heterogeneous Catalysis. New York: VCH Publishers Inc., 1997.

United States Environmental Protection Agency (US EPA), "Use of Monitoring Natural Attenuation at Superfund, RCRA Corrective Action, and Underground Storage Tank Sites," Office of Solid Waste and Emergency Response Directive 9200.4-17, 1997.

Vogel, T. M. and P.L. McCarty, "Biotransformation of Tetrachloroethylene to Trichloroethylene, Dichloroethylene, Vinyl Chloride, and Carbon Dioxide under Methanogenic Conditions," Applied and Environmental Microbiology, 49(5): 2723-2725, 1985.

VITA

Capt Chris M. Stoppel was born [redacted] in Dodge City, KS. He grew up in Scott City, KS and graduated from Scott Community High School in 1992. He then entered the United States Air Force Academy in Colorado Springs, Colorado to commence his undergraduate studies. He graduated with a Bachelor of Science degree in Civil Engineering and was commissioned as an Air Force officer on 29 May 1996. In August 1999, he entered the Graduate Engineering and Environmental Management program of the Graduate School of Engineering and Management, Air Force Institute of Technology.

REPORT DOCUMENTATION PAGE

Form Approved
OMB No. 074-0188

1. REPORT DATE *(DD-MM-YYYY)*	2. REPORT TYPE	3. DATES COVERED *(From – To)*
20-03-2001	Master's Thesis	Sep 1999 – Feb 2001

4. TITLE AND SUBTITLE

A MODEL FOR PALLADIUM CATALYZED DESTRUCTION OF CHLORINATED ETHENES IN CONTAMINATED GROUNDWATER

5a. CONTRACT NUMBER

5b. GRANT NUMBER

5c. PROGRAM ELEMENT NUMBER

6. AUTHOR(S)

Chris M. Stoppel, Capt, USAF

5d. PROJECT NUMBER
NA

5e. TASK NUMBER

5f. WORK UNIT NUMBER

7. PERFORMING ORGANIZATION NAMES(S) AND ADDRESS(S)

Air Force Institute of Technology
Graduate School of Engineering and Management (AFIT/EN)
2950 P Street, Building 640
WPAFB OH 45433-7765

8. PERFORMING ORGANIZATION REPORT NUMBER

AFIT/GEE/ENV/01M-21

9. SPONSORING/MONITORING AGENCY NAME(S) AND ADDRESS(ES)

Air Force Center for Environmental Excellence/Technology Transfer Division
Attn: Maj Jeff S. Cornell
3207 North Road, Building 532
Brooks AFB TX 78235-5357 (210) 536-4329

10. SPONSOR/MONITOR'S ACRONYM(S)
AFCEE/ERT

11. SPONSOR/MONITOR'S REPORT NUMBER(S)

12. DISTRIBUTION/AVAILABILITY STATEMENT

APPROVED FOR PUBLIC RELEASE; DISTRIBUTION UNLIMITED.

13. SUPPLEMENTARY NOTES

14. ABSTRACT

Groundwater contamination by chlorinated ethenes is a widespread environmental problem. Conventional remediation technologies have shortcomings that have prompted further research into the development of novel treatment technologies. A palladium/alumina catalyst in the presence of dissolved molecular hydrogen (referred to hereafter as a Pd/H_2 system) has been demonstrated to rapidly destroy chlorinated ethene contaminated groundwater. First-order kinetics have been used to model chlorinated ethene destruction in a Pd/H_2 reactor. However, catalyst deactivation and regeneration are important processes that also need to be modeled in order to better understand their effect on treatment efficiency. This study presents a model for palladium catalyzed destruction of chlorinated ethenes that includes catalyst deactivation and regeneration. The model is validated using published column experiment results performed at Stanford University. The model is then coupled with an analytical groundwater flow model to simulate application of in-well Pd/H_2 reactors to accomplish subsurface contaminant destruction in a Horizontal Flow Treatment Well (HFTW) system. Applying the model under realistic conditions results in approximately 130 days of system operation without significant catalyst deactivation. This suggests catalyst deactivation may not significantly affect operating costs or system performance in a real remediation scenario. The model presented in this study, by incorporating the relevant processes of catalyst deactivation and regeneration, represents an important step in transitioning the Pd/H_2 in-well system toward field application.

15. SUBJECT TERMS

Groundwater contamination, palladium catalyst, chlorinated ethenes, first-order kinetics, catalyst deactivation, catalyst regeneration

16. SECURITY CLASSIFICATION OF:			17. LIMITATION OF ABSTRACT	18. NUMBER OF PAGES	19a. NAME OF RESPONSIBLE PERSON
a. REPORT	b. ABSTRACT	c. THIS PAGE			Professor Mark N. Goltz, ENV
U	U	U	UU	96	19b. TELEPHONE NUMBER *(Include area code)* (937) 255-3636, ext 4638

Standard Form 298 (Rev. 8-98)
Prescribed by ANSI Std. Z39-18

Form Approved
OMB No. 074-0188